Colloquium: Fracton matter

Andrey Gromov*

Department of Physics and Condensed Matter Theory Center, University of Maryland, College Park, Maryland 20742, USA

Leo Radzihovsky†

Department of Physics and Center for Theory of Quantum Matter, University of Colorado, Boulder, Colorado 80309, USA

(published 5 January 2024)

The burgeoning field of "fractons," a class of models where quasiparticles are strictly immobile or display restricted mobility that can be understood through generalized multipolar symmetries and associated conservation laws, is reviewed. With a focus on merely a corner of this fast-growing subject, it is demonstrated how one class of such theories, symmetric tensor and coupled-vector gauge theories, surprisingly emerge from familiar elasticity of a two-dimensional quantum crystal. The disclination and dislocation crystal defects, respectively, map onto charges and dipoles of the fracton gauge theory. This fracton-elasticity duality leads to predictions of fractonic phases and quantum phase transitions to their descendants that are duals of the commensurate crystal, supersolid, smectic, and hexatic liquid crystals, as well as amorphous solids, quasicrystals, and elastic membranes. It is shown how these dual gauge theories provide a field-theoretic description of quantum melting transitions through a generalized Higgs mechanism. It is demonstrated how they can be equivalently constructed as gauged models with global multipole symmetries. Extensions of such gauge-elasticity dualities to generalized elasticity theories are expected to provide a route to the discovery of new fractonic models and their potential experimental realizations.

DOI: 10.1103/RevModPhys.96.011001

CONTENTS

*andrey@umd.edu
†radzihov@colorado.edu

I. INTRODUCTION AND MOTIVATION

Characterization and classification of phases of matter and the phase transitions between them is a central pursuit of condensed matter physics. The simplest and most ubiquitous organization of matter is according to Landau's symmetry-breaking paradigm. Such phases [crystals, magnets, superfluids, a panoply of liquid crystal phases, and many others (De Gennes and Prost, 1993; Chaikin and Lubensky, 1995; Kleman and Lavrentovich, 2003)] are distinguished by

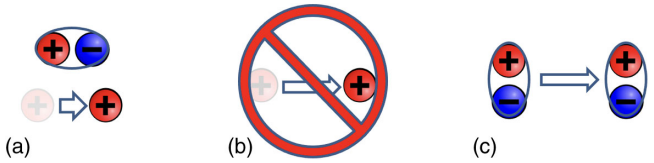

FIG. 1. (a) Illustration of dipole conservation enforcing (b) the immobility of the fractonic charges with dipole conservation. (c) Subdimensional mobility of a dipole.

patterns of spontaneous symmetry breaking that are characterized by a local order parameter and a short-range entangled, nearly product many-body wave function.[1]

Stimulated by an ever-growing class of unusual quantum materials that appear to lie outside of these Landau symmetry-breaking and Fermi liquid paradigms, much effort has been directed at exploring models that exhibit quantum phases with fractionalized anyonic quasiparticles, robust spectral degeneracy sensitive only to the topology of space, and other unusual properties common to the so-called topological quantum liquids (Savary and Balents, 2017). Such exotic phenomenology is captured by conventional gauge theories, where fractionalized quasiparticles appear at the ends of effective field lines, free to move by growing the corresponding tensionless string, much like charges in Maxwell's electrodynamics.

Motivated by a continued interest in topological quantum matter, by quantum glasses, and by a search of fault-tolerant quantum memory, more recently researchers have discovered a new class of theoretical models. These feature system-size-dependent ground-state degeneracy, gapped quasiparticles with restricted mobility,[2] and many other highly unusual properties; see Fig. 1. The first, and most well-known, example is the strictly immobile excitation, named a fracton. Fractons and other subdimensional particles (lineons and planeons, restricted to move in one and two dimensions) were originally discovered in fully gapped models of commuting projector (stabilizer code) lattice spin Hamiltonians (Chamon, 2005; Bravyi, Leemhuis, and Terhal, 2011b; Haah, 2011, 2013a, 2013b, 2016; Castelnovo and Chamon, 2012; Bravyi and Haah, 2013; Yoshida, 2013; Vijay, Haah, and Fu, 2015, 2016), which were recently reviewed by Pai and Pretko (2018), Nandkishore and Hermele (2019), Pretko, Chen, and You (2020), and Grosvenor *et al.* (2022).[3]

These fractonic models challenge our understanding of the relationship between phases of matter and quantum field theories (QFTs) for a number of reasons (Qi, Radzihovsky, and Hermele, 2021). For instance, until recently it was conventional wisdom that any gapped phase of matter has a low-energy topological QFT (TQFT) description. However, gapped fracton phases have a robust ground-state degeneracy where on a spatial d torus the dimension of the ground-state degeneracy grows exponentially with system size[4] (Bravyi, Leemhuis, and Terhal, 2011b; Haah, 2011, 2013a). This is incompatible with a TQFT description. The absence of a continuum field theory description for the Haah model can also be seen from the bifurcating nature of the renormalization group flow (Haah, 2014). There is, however, a description in terms of TQFT supplemented with a defect network (Aasen *et al.*, 2020; Wen, 2020). Moreover, the number of superselection sectors (i.e., distinct types of particlelike excitations) also diverges (Haah, 2013b, 2016; Pai and Pretko, 2018). This is suggestive of an infinite number of fields required in the continuum, with a nontrivial dependence on lattice scale, i.e., no obvious continuum field theory limit.

More recently it was realized that (even if incomplete) such exotic excitations have a natural theoretical description in the language of higher-rank symmetric tensor gauge theories and complementary coupled-vector gauge theories, which exhibit restricted mobility due to an unusual set of higher (for example, dipole) moment charge conservation (Pretko, 2017a, 2017b, 2018; Pretko and Radzihovsky, 2018a; Gromov, 2019a; Pretko, Zhai, and Radzihovsky, 2019; Radzihovsky and Hermele, 2020). In contrast to the aforementioned models, which are based on discrete symmetries, this class of $\mathrm{U}(N)$ fractonic tensor gauge theories exhibits gapless degrees of freedom. These are related to discrete models through a condensation of higher charge matter (Bulmash and Barkeshli, 2018a; Ma, Hermele, and Chen, 2018). Rapid recent progress in the field has established connections with numerous other areas of physics, such as localization (Prem, Haah, and Nandkishore, 2017; Pretko, 2017c; Pai, Pretko, and Nandkishore, 2019), gravity (Pretko, 2017d), holography (Yan, 2019), quantum Hall systems (Doshi and Gromov, 2021; Du *et al.*, 2022), and deconfined quantum criticality (Ma and Pretko, 2018), among many other theoretical developments (Xu and Horova, 2010; Williamson, 2016; Albert, Pascazio, and Devoret, 2017; Halász, Hsieh, and Balents, 2017; Hsieh and Halász, 2017; Ma *et al.*, 2017, 2018; Pretko, 2017e; Shi and Lu, 2017; Slagle and Kim, 2017a, 2017b; Vijay, 2017; Vijay and Fu, 2017; Devakul, Parameswaran, and Sondhi, 2018; He *et al.*, 2018; Prem, Pretko, and Nandkishore, 2018; Shirley, Slagle, and Chen, 2019; Slagle, Prem, and Pretko, 2019; Bidussi *et al.*, 2022; Jain and Jensen, 2022).

While exotic properties of fractons have been a subject of intense study, concrete physical realizations have been lacking. However, it was recently demonstrated explicitly through dualities (Kleinert, 1983) between quantum elasticity and $\mathrm{U}(1)$ symmetric tensor (Pretko and Radzihovsky, 2018a, 2018b; Gromov, 2019b, 2020; Kumar and Potter, 2019; Pretko, Zhai, and Radzihovsky, 2019; Gromov and Surowka, 2020; Nguyen, Gromov, and Moroz, 2020; Radzihovsky, 2020; Zhai and Radzihovsky, 2021) and coupled-vector gauge

[1]Fermionic phases are more challenging, with the simplest and best understood one being Landau's Fermi liquid.

[2]No local operator can move an isolated excitation in one or more spatial directions (or all of them) without creating additional excitations.

[3]There are two qualitatively distinct classes of models with restricted mobility. As discussed in Sec. IV, one class is with highly fragile, fine-tuned global multipolar and subsystem symmetries. The other class is gaugelike theories with topological order that are generally robust over some nonzero range of all local perturbations.

[4]Gapped, topologically ordered fracton models can appear only in dimensions $d > 2$. (Aasen *et al.*, 2020; Haah, 2021).

theories[5] (Radzihovsky and Hermele, 2020; Qi, Radzihovsky, and Hermele, 2021) that the fracton phenomena is realized as topological defects in two-dimensional quantum crystals, supersolids, and smectics. In this Colloquium we review the physics of gapless fractons, with a particular focus on the application of fractons and corresponding fractonic gauge theories to real physical systems. In Sec. II we define and discuss in a model-independent way the unifying properties of fractonic quasiparticles. The central component of the Colloquium appears in Sec. III, where we present dualities between various quantum elastic systems, such as crystals, supersolids, and liquid crystals, and their fractonic gauge theories. In Sec. IV we utilize these gauge-theoretic descriptions to discuss phase transitions between these quantum phases of matter, and most notably a gauge-theoretic formulation of quantum melting. A variety of field-theoretic constructions that give rise to gapless and gapped fracton phases are summarized and reviewed in Sec. V. Synthesis, open questions, and future directions are relegated to the end of Sec. V.

II. GENERAL PERSPECTIVE ON RESTRICTED MOBILITY

As we see throughout the Colloquium, fracton excitations emerge in a wide variety of much different physical systems. Consequently, it is useful to decouple the phenomenon of restricted mobility of excitations from a specific model or a physical origin that enforces it. Thus, in this section we present a general, realization-independent formulation of excitations with restricted mobility, taking a symmetry-based approach. In all systems that we consider it is assumed that the total number (or charge) of the fractons is conserved. The conservation can be either exact, implemented by a U(1) symmetry, or partially broken, implemented by a symmetry-breaking pattern $\mathrm{U}(1) \to \mathbb{Z}_p$. We start with the former.

A global U(1) symmetry implies the continuity equation

$$\partial_0 \rho + \partial_i J^i = 0 \Rightarrow \partial_0 Q = 0, \tag{1}$$

where ρ is the fracton density, J^i is the fracton current, and $Q(t) = \int d^d x \rho(t, \mathbf{x})$ is the total charge. In a seminal paper Pretko (2017a) showed that the mobility of charges is restricted by further enforcing the conservation of multipole moments $Q_{i_1 i_2 \cdots i_n}$ of the charge density,

$$Q_{i_1 i_2 \cdots i_n} = \int d^d x \, x_{i_1} x_{i_2} \cdots x_{i_n} \rho(\mathbf{x}). \tag{2}$$

To enforce such a conservation law we demand the current to be of a special form,

$$J^i = \partial_{i_1} \partial_{i_2} \cdots \partial_{i_n} J^{i_1 i_2 \cdots i_n i}, \tag{3}$$

where $J^{i_1 i_2 \cdots i_n i}$ is a symmetric tensor of rank $n+1$. It describes the transport of the nth multipole moment $Q_{i_1 i_2 \cdots i_n}$ in the direction $\hat{x}_i$. Combining Eqs. (1)–(3), we find that all multipole moments up to the nth moment are conserved (assuming that all fields decay to 0 at infinity)

$$\partial_0 Q_{i_1 i_2 \cdots i_k} = 0, \qquad k \le n. \tag{4}$$

Conservation law (4) implies restricted mobility because generic motion of the charges will change the multipole moment of the system. The symmetry leading to these conservation laws is an extension of spatial symmetries named the multipole algebra and has nontrivial commutation relations with generators of rotation and translations (Gromov, 2019a). Tensor and coupled-vector gauge theories discussed later emerge upon gauging this symmetry.

To make this generic formulation more concrete, we consider a theory with a conserved dipole moment Q_i and examine its two fracton excitations of equal and opposite charge located at $\mathbf{x}_1$ and $\mathbf{x}_2$. Let $T_i(\mathbf{a}_i)$ be an operator that translates the ith fracton by vector $\mathbf{a}_i$. Dipole conservation then implies

$$\langle \mathbf{x}_1, \mathbf{x}_2 | T_1(\mathbf{a}_1) T_2(\mathbf{a}_2) | \mathbf{x}_1, \mathbf{x}_2 \rangle \propto \delta^{(d)}(\mathbf{a}_1 - \mathbf{a}_2). \tag{5}$$

The same conclusion can also be reached directly from the constraint on the current $J^i = \partial_j J^{ji}$. For simplicity, focusing on two dimensions we consider a wide strip extended in the $\hat{x}_2$ direction and assume that the system is in a homogeneous steady state. The total charge current flowing through a cross section of a strip in the $\hat{x}_1$ direction is

$$J^i_{\mathrm{tot}} = \int_{-\infty}^{\infty} dx_2 (\partial_1 J^{1i} + \partial_2 J^{2i}) = \partial_1 \int_{-\infty}^{\infty} dx_2 J^{1i} = 0, \tag{6}$$

where in the last step we used homogeneity. Indeed, if the charges can move around only in the form of bound dipoles, the total current through any cross section in a homogeneous state will always be 0.

Complementarily we can define a microscopic dipole current $\tilde{J}^{ij} = x^i J^j$, with the dipole density ρ^i satisfying

$$\partial_0 \rho^i + \partial_j \tilde{J}^{ij} = J^i. \tag{7}$$

Equation (7) demonstrates that the motion of monopoles ($J^i \neq 0$) generates dipoles, thereby violating their continuity equation, and equivalently dipole conservation demands a vanishing of the monopole current, $J^i = 0$, i.e., immobility of fractonic monopoles (Radzihovsky, 2020; Radzihovsky and Hermele, 2020).

The previously discussed conservation laws do not cover the variety of mobility-constrained systems. There are two important generalizations that one has to consider. First, Eq. (3) assumes that the tensor current transforms in a representation of SO(d). Since most systems supporting fractons are initially formulated on a lattice, there is no *a priori* reason for SO(d) symmetry to be relevant. Indeed, the current may transform in representations of a point group symmetry. This is crucial to fit lattice models with discrete symmetries, like the X-cube, Chamon, and Haah codes, into this framework. Second, the charge density ρ itself can be assumed to be a tensor transforming in some representation of either SO(d) or its point subgroup. In this case the relevant multipole moments are the elementary excitations and cannot be further divided into smaller moments or point charges. Finally, when the charge conservation is broken down to $\mathbb{Z}_p$,

[5]The latter admit high-dimensional and lattice generalizations.

the multipole conservation still imposes modulo-p constraints on the system. However, a general theory of such systems has not yet been developed.

III. FRACTONS AS CRYSTALLINE DEFECTS

In this section we describe an interesting connection of fractonic dynamics to the restricted mobility of positional topological defects (dislocations) and orientational topological defects (disclinations) in a familiar quantum two-dimensional crystal (Pretko and Radzihovsky, 2018a, 2018b; Gromov, 2019b; Pretko, Zhai, and Radzihovsky, 2019; Radzihovsky and Hermele, 2020). Thus, a quantum crystal has provided the only known physical realization of a fractonic system to date. Building on this we further show here how the corresponding coupled U(1) vector and the equivalent symmetric tensor gauge theories provide a theory of quantum melting of a crystal and discuss intermediate liquid crystal phases. This section introduces the main ideas from the theory of particles with restricted mobility as well as tensor and multipole gauge theories.

A. Particle-vortex duality

As a warm-up for fractonic duality of crystals and liquid crystals, we review the standard $(2+1)$D particle vortex or, equivalently,[6] XY-to-Abelian-Higgs model duality (Peskin, 1978; Dasgupta and Halperin, 1981; Fisher and Lee, 1989).

The low-energy effective Lagrangian describing $(2+1)$D bosons is given by[7]

$$\mathcal{L} = \frac{K}{2}(\partial_\mu \phi)^2, \tag{8}$$

where ϕ is the superfluid phase and we used the units in which the speed of sound is 1. In the presence of vortices, the boson current $\partial_\mu \phi$ can be decomposed into smooth and singular vortex parts $\partial_\mu \phi = \partial_\mu \phi_s + v_\mu$. The circulation of the latter

$$\epsilon^{\mu\nu\rho}\partial_\nu v_\rho \equiv (\partial \times v)^\mu = j^\mu_v \tag{9}$$

gives the vortex 3-current $j^v_\mu = (\rho^v, j^v_i)$.

Introducing a Hubbard-Stratonovich field J_μ transforms the Lagrangian (8) into

$$\mathcal{L} = \frac{K^{-1}}{2} J_\mu J^\mu + (\partial_\mu \phi_s + v_\mu) J^\mu. \tag{10}$$

Integrating out the smooth component of ϕ enforces the boson continuity equation

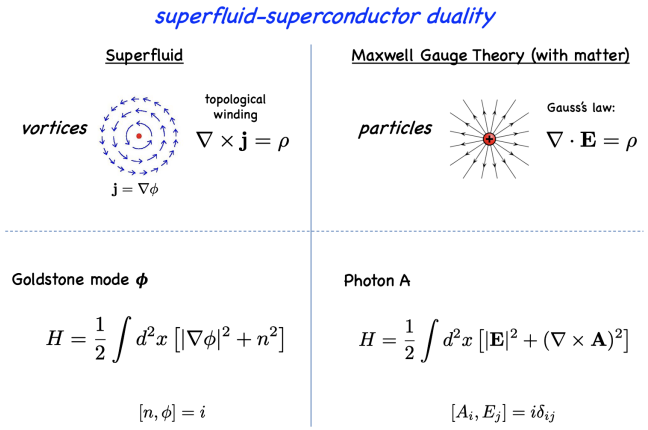

FIG. 2. Boson-vortex duality in a $(2+1)$D XY model (also known as superfluid-superconductor duality), whose tensor generalization is the fracton-disclination (gauge-elasticity) duality summarized in Fig. 3.

$$\partial_\mu J^\mu = 0, \tag{11}$$

which is solved in terms of a vector potential $J^\mu = \epsilon^{\mu\nu\rho}\partial_\nu A_\rho = (\partial \times A)^\mu$, with the physical current invariant under a gauge transformation

$$\delta A_\mu = \partial_\mu \chi. \tag{12}$$

The Lagrangian (8) then takes the form of a U(1) gauge theory,

$$\begin{aligned}\tilde{\mathcal{L}} &= \frac{K^{-1}}{2}(\partial \times A)^2 + j^\mu_v A_\mu \\ &= \frac{K^{-1}}{2}(E^2 - B^2) + j^\mu_v A_\mu,\end{aligned} \tag{13}$$

where the electric field $E_i = \partial_0 A_i - \partial_i A_0$ and the magnetic field $B = \epsilon^{ij}\partial_i A_j$, respectively, describe the spatial components of bosonic current and number densities, and under the duality the vortex 3-current j^μ_v enters Lagrangian as the dual matter.

In an equivalent Hamiltonian description that is illustrated in Fig. 2, bosons are described by

$$\hat{\mathcal{H}} = \tfrac{1}{2}|\boldsymbol{\nabla}\hat{\phi}|^2 + \tfrac{1}{2}\hat{\rho}^2 \tag{14}$$

in terms of canonically conjugate $[\hat{\rho}, \hat{\phi}] = i\delta^{(2)}(\mathbf{x})$ and vortex singularities $\boldsymbol{\nabla} \times \boldsymbol{\nabla}\phi = \rho_v$. On the dual side, rotating the boson current $\boldsymbol{\nabla}\phi$ lines by $\pi/2$ transforms them into electric field lines $\mathbf{E}$ and boson density into dual flux density $\mathbf{B}$, with $[\hat{\mathbf{A}}, \hat{\mathbf{E}}] = i\delta^{(2)}(\mathbf{x})$. This then transforms the bosonic Hamiltonian into the dual Maxwell theory

$$\tilde{\hat{\mathcal{H}}} = \tfrac{1}{2}|\hat{\mathbf{E}}|^2 + \tfrac{1}{2}(\boldsymbol{\nabla} \times \hat{\mathbf{A}})^2 - \mathbf{j}_v \cdot \mathbf{A}. \tag{15}$$

It is more formally obtained from the dual Lagrangian (13) by introducing an independent electric field $\mathbf{E}$ as the

[6] It is also known as a duality between a superfluid and a superconductor.

[7] The XY model Lagrangian and its duality can be treated more carefully on a lattice, giving equivalent results. Thus, our streamlined continuum approach is fundamentally justified by lattice regularization.

Hubbard-Stratonovich field to decouple the spatial (electric field energy) part of the Maxwell term. Integration over the time component A_0 then gives the Gauss law

$$\boldsymbol{\nabla}\cdot\mathbf{E}=\rho_v, \tag{16}$$

which generates Eq. (12) and is the dual counterpart of the circulation constraint [Eq. (9)].

We thus recover the well-known Dasgupta-Halperin duality (Peskin, 1978; Dasgupta and Halperin, 1981; Fisher and Lee, 1989), where a bosonic liquid is dual to vortex matter, described by a complex scalar field Ψ minimally coupled to a U(1) gauge field A_μ,

$$\mathcal{L}=i\Psi^\star(\partial_0-iA_0)\Psi-\frac{1}{2m}|(\partial_i-iA_i)\Psi|^2+V(|\Psi|)+\frac{K^{-1}}{2}(\partial\times A)^2. \tag{17}$$

It is also known as the Abelian-Higgs model of a dual superconductor, with V a generic U(1)-symmetric potential. In this duality, a superfluid and Mott-insulating phase of bosons thus, respectively, correspond to a dual-normal (dual-nonsuperconducting, $\Psi=0$) state and a dual-superconducting vortex condensate ($\Psi\neq 0$ dual-Higgs) phase.

B. Fracton-disclination duality: Commensurate crystal

1. Tensor gauge theory duality

The duality of an elastic medium is a technically straightforward tensor generalization (Kleinert, 1983, 1989, 2008; Beekman *et al.*, 2017) of the aforementioned *XY* duality, where the phonons u_i, the dislocations, and the disclinations are respective vector counterparts of the superfluid phase ϕ and vortices. Since a 2D elastic medium is described by phonon Goldstone modes that are spatial vectors, it is not surprising that their dual is captured by a tensor (rather than a vector) gauge field[8] A_{ij}.

To this end (Pretko and Radzihovsky, 2018a, 2018b; Pretko, Zhai, and Radzihovsky, 2019), we begin with a low-energy elastic description of a $(2+1)$-dimensional quantum crystal captured by a harmonic Lagrangian

$$\mathcal{L}=\tfrac{1}{2}(\partial_0 u_i)^2-\tfrac{1}{2}C^{ijkl}u_{ij}u_{kl}, \tag{18}$$

where $u_{ij}=(1/2)(\partial_i u_j+\partial_j u_i)$ is the linearized symmetric strain tensor (encoding target-space rotational invariance), the rank-4 tensor C^{ijkl} encodes elastic moduli and underlying crystal symmetry, and we specialized to unit mass density (Chaikin and Lubensky, 1995). To include topological defects, we express the displacement in terms of smooth phonon and singular defect components $u_i=u_i^{\mathrm{s}}+u_i^{\mathrm{d}}$, with the latter accounting for the disclination density ρ,

$$\epsilon^{ik}\epsilon^{j\ell}\partial_i\partial_j u_{k\ell}=\rho, \tag{19}$$

and implicitly for dislocations as they are dipole bound states of two disclinations (Landau, Lifshitz, and Kosevich, 1986; Seung and Nelson, 1988; Chaikin and Lubensky, 1995). Introducing the Hubbard-Stratonovich momentum π^i and symmetric stress σ^{ij} fields and integrating over the phonons u_i^{s} enforces the momentum continuity $\partial_0\pi^i+\partial_j\sigma^{ij}=0$. To make contact with electromagnetism, it is convenient to introduce dual vector magnetic ($B_i=\epsilon^{ij}\pi_j$) and symmetric tensor electric ($E_\sigma^{ij}=\epsilon^{ik}\epsilon^{jl}\sigma_{kl}$) fields in terms of which the momentum continuity equation takes the form of a generalized Faraday law

$$\partial_0 B^i+\epsilon_{jk}\partial^j E_\sigma^{ki}=0 \tag{20}$$

of the scalar-charge tensor gauge theory (Pretko, 2017a). As in conventional electromagnetism, the latter can be solved in terms of gauge fields, here the symmetric tensor A_{ij} and scalar A_0,

$$B_i=\epsilon^{kl}\partial_k A_{li},\qquad E_\sigma^{ij}=-\partial_0 A^{ij}+\partial^i\partial^j A_0, \tag{21}$$

which are invariant under the gauge transformations

$$\delta A_{ij}=\partial_i\partial_j\chi,\qquad \delta A_0=\partial_0\chi. \tag{22}$$

The elasticity Lagrangian (18) then takes on the Maxwell-like form

$$\mathcal{L}=\tfrac{1}{2}\tilde{C}_{ijkl}E^{ij}E^{kl}-\tfrac{1}{2}B^2+\rho A_0-J^{ij}A_{ij}, \tag{23}$$

where $\tilde{C}^{-1}_{ijkl}=C^{-1}_{mnpq}\epsilon_i{}^m\epsilon_j{}^n\epsilon_k{}^p\epsilon_l{}^q$ and $E_{ij}=\tilde{C}^{-1}_{ijkl}E_\sigma^{kl}$. The dual gauge fields are sourced by crystalline topological defects through the last two terms in Eq. (23), with the dislocation current given by

$$J^{ij}=\epsilon^{ik}\epsilon^{j\ell}(\partial_0\partial_k-\partial_k\partial_0)u_\ell, \tag{24}$$

where J^{ij} corresponds to a dipole p^i (a $\pi/2$ rotated Burgers vector) moving in the j direction. Gauge invariance (22) requires that the dual charge and current densities ρ and J^{ij} satisfy the continuity equation

$$\partial_0\rho+\partial_i\partial_j J^{ij}=0, \tag{25}$$

with a current constrained in the manner discussed in Sec. II, as required on general grounds. Notably the immobility of fractonic disclination charges ρ is reflected in the absence (vanishing) of the fracton current. Gauss's law generating the gauge transformations (22) can be read out from Eqs. (21) and (23), appears as a constraint after integration over the scalar potential A_0, and takes the form

$$\partial_i\partial_j E^{ij}=\rho. \tag{26}$$

Equation (26) is the counterpart of the topological disclination condition (19), as illustrated in Fig. 3.

For an isotropic crystal, the elastic tensor C_{ijkl} reduces to two independent Lamé moduli μ and λ, and dual Maxwell-like theory (23) exhibits 2 propagating gapless degrees of freedom corresponding to transverse and longitudinal

[8]See, however, Sec. III.B.4 for the coupled U(1) vector gauge theory formulation of the elasticity dual at low energies equivalent to the tensor gauge theory presented in this section.

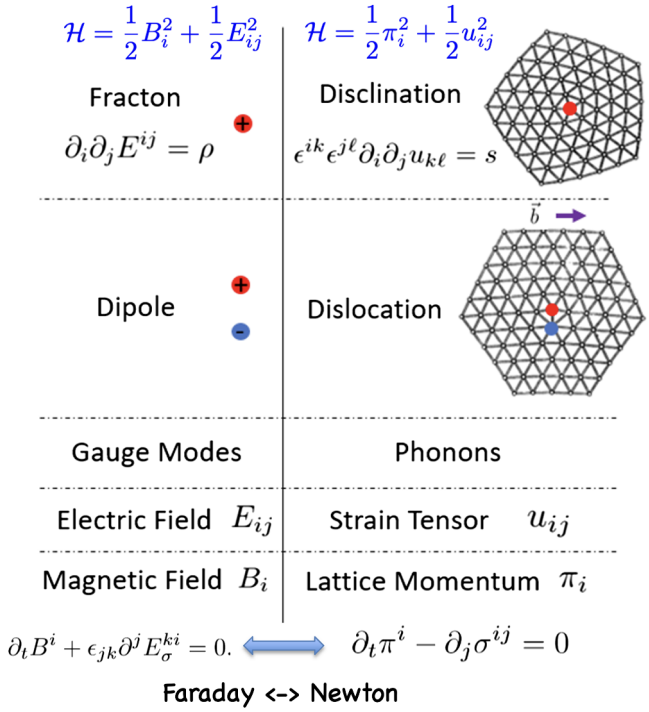

FIG. 3. Fracton-elasticity dictionary. The topological defects, phonons, and strains of a two-dimensional quantum crystal (right column) are in a one-to-one relation with the charges, gauge fields, and fields of the scalar-charge rank-2 tensor gauge theory (left column).

phonons. This demonstrates that a quantum crystal is dual to so-called traceless scalar-charge gauge theory (Pretko and Radzihovsky, 2018a, 2018b; Gromov, 2019b; Pretko, Zhai, and Radzihovsky, 2019) and gives the only known physical realization of fractonic matter.

As further discussed in Sec. III.E, we note that a conservation of the number of occupied lattice sites, i.e., the absence of vacancy and interstitial point defects, characteristic of a "commensurate" crystal implies that J^{ij} is traceless (since the trace J^{ii} corresponds to dipole motion along its orientation, which is forbidden by atom conservation) and further constrains the motion of defects (Pretko and Radzihovsky, 2018b; Kumar and Potter, 2019; Pretko, Zhai, and Radzihovsky, 2019). Equation (25) then implies that the total dual charge, dipole moment, and trace of the quadrupole moment are conserved,

$$\partial_0 Q = 0, \quad \partial_0 Q_i = 0, \quad \partial_0 \mathrm{tr}(Q_{ij}) = 0. \tag{27}$$

Identification of the charges, dipoles, and quadrupoles of this fracton phase $\mathrm{F}_{\mathrm{U}(1)}$ with disclinations, dislocations (with a Burgers vector perpendicular to the dipole moment), and vacancies and interstitials (Pretko and Radzihovsky, 2018b; Gromov, 2019b; Kumar and Potter, 2019; Pretko, Zhai, and Radzihovsky, 2019) gives an effective gauge theory formulation of their quantum dynamics in a commensurate crystal. Namely, the fracton charges encode the immobility of disclinations, the duality prediction (Pretko and Radzihovsky, 2018a) that can also be understood directly in terms of crystal

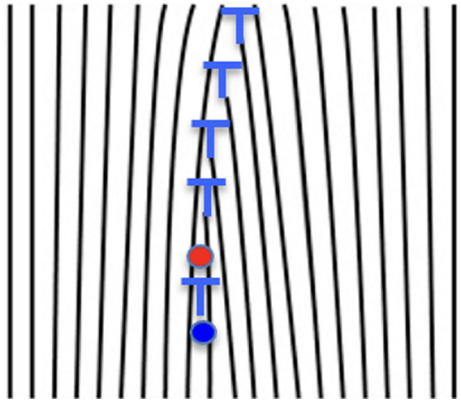

FIG. 4. Instantiation of an immobile fracton as a disclination defect of a $(2+1)$D crystal. When a disclination as an end point of a ray of dislocation dipoles is viewed, its hop by a lattice constant [from the first (red) to the second (blue) dot] corresponds to the addition of a dislocation dipole. Since the latter corresponds to an addition of a half ray of atoms, this highly nonlocal operator is not allowed in a local Hamiltonian (and not just by a global symmetry), thereby strictly forbidding disclination motion.

degrees of freedom, as illustrated in Fig. 4. The lineon dipoles, with motion constrained [by the $\mathrm{U}(1)$ conservation of the trace of quadrupoles in Eq. (27)] transverse to the dipole moment, correspond to the well-known *glide-only constraint* that, in the absence of vacancies and interstitials, prevents dislocations from *climbing* perpendicular to their Burgers vector (Pretko and Radzihovsky, 2018b; Gromov, 2019b; Kumar and Potter, 2019; Pretko, Zhai, and Radzihovsky, 2019), as illustrated in the top sketches in Fig. 5. In Sec. III.E, we further discuss the relaxation of this $\mathrm{U}(1)$ symmetry-enriched constraint, which leads to a qualitatively distinct fractonic state F, which corresponds to an *incommensurate* crystal, i.e., a supersolid.

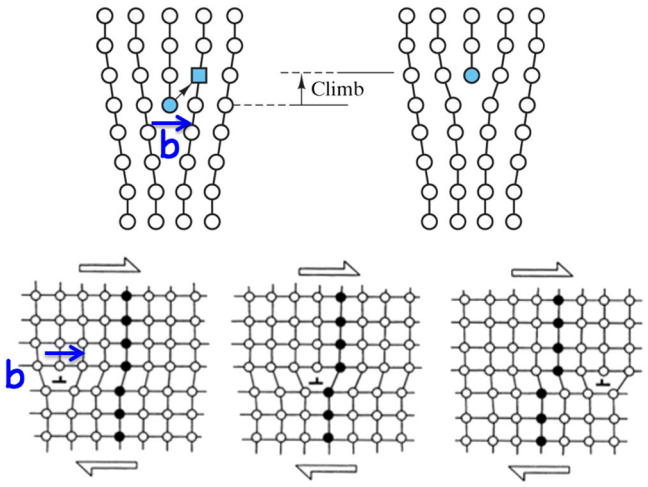

FIG. 5. Top illustration: a dislocation climb transverse to the Burgers vector **b** (motion of a dipole along the dipole) that is forbidden by charge conservation but made possible by a nonzero density of vacancies and interstitials. Bottom illustration: the allowed dislocation lineon glide motion along **b** (transverse to the dipole).

2. Disclination field theory

With crystalline defects appearing as dual matter that sources tensor gauge fields, the formulation extends to a concrete field-theoretic representation of fractonic matter ρ and J^{ij}. To this end, we describe disclinations by a complex scalar field Φ, treating them as bosonic excitations. The Lagrangian $\mathcal{L}=\mathcal{L}_s[A_{ij},\Phi]+\mathcal{L}_{\mathrm{Max}}[A_{ij}]$ is a sum of the dual disclination matter sector $\mathcal{L}_s$ and the Maxwell-like sector $\mathcal{L}_{\mathrm{Max}}$, which were derived in Sec. III.B.1 and capture the phonon degrees of freedom. The dual matter Lagrangian $\mathcal{L}_s$ takes the form (Pretko, 2018)

$$\mathcal{L}_s = i\Phi^*(\partial_0 - iA_0)\Phi + g[|D_1(\Phi)|^2 + |D_2(\Phi)|^2] + V(\Phi), \tag{28}$$

where $D_I(\Phi)$ are differential operators, bilinear in Φ, given by

$$D_I(\Phi) = \Pi_I^{ij}(\partial_i\Phi\partial_j\Phi - \Phi\partial_i\partial_j - iA_{ij}\Phi), \qquad \vec{\Pi} = (\sigma_1,\sigma_3), \tag{29}$$

where σ_1 and σ_3 are the Pauli matrices. In the absence of gauge fields, the Lagrangian (28) exhibits a conservation law (25) due to the presence of an unusual "global" symmetry,

$$\Phi' = e^{i\chi_g(\mathbf{x})}\Phi, \qquad \chi_g(\mathbf{x}) = \alpha + \beta_i x^i + \tfrac{1}{2}\gamma|x|^2, \tag{30}$$

characterized by the phase $\chi_g(\mathbf{x})$, which by the virtue of Noether's theorem leads to the conservation of the U(1) charge, dipole, and trace of the quadrupole moments. In the presence of tensor gauge fields transforming according to Eq. (22), the Lagrangian (28) is also invariant under a general gauge transformation $\Phi \to e^{i\chi(\mathbf{x})}\Phi$ with an arbitrary $\chi(\mathbf{x})$. As in conventional gauge theories, here the disclination density and dislocation current are given as variational derivatives

$$\rho = \frac{\delta S}{\delta A_0}, \qquad J^{ij} = \frac{\delta S}{\delta A_{ij}}. \tag{31}$$

It follows from Eq. (29) that the current J^{ij} is indeed traceless, as expected.[9]

3. Dislocation field theory

The kinetic energy of the aforementioned disclination field theory $\mathcal{L}_s$ is quartic in the fields and thus does not admit a weak-coupling quadratic representation, thereby reflecting its strongly interacting UV degrees of freedom. Indeed, in real crystals disclinations appear in tightly bound lattice-scale dislocation dipoles. To construct their field theory $\mathcal{L}_d$, we observe that a dislocation with a Burgers vector $\mathbf{b}$ (an elementary lattice vector) is created by an operator $\psi^\dagger_{\mathbf{d}}$ labeled as the disclination dipole $\mathbf{d}$ (corresponding to the ρ_i density of Sec. II and $\mathbf{p}$ in the following), with the corresponding coherent state field

$$\psi^*_{\mathbf{d}}(\mathbf{x}) = \Phi\left(\mathbf{x}-\frac{\mathbf{d}}{2}\right)\Phi^*\left(\mathbf{x}+\frac{\mathbf{d}}{2}\right), \tag{32}$$

and is bilocal in the disclination fields, with $\mathbf{b}=\mathbf{d}\times\hat{\mathbf{z}}$. Under the global symmetry (30), in the $d\to 0$ limit the dipole operator transforms as

$$\psi_{\mathbf{d}}(\mathbf{x}) \to e^{i\beta_i d^i + i\gamma d_i x^i}\psi_{\mathbf{d}}(\mathbf{x}), \tag{33}$$

where the first factor is a global phase enforcing U(1) symmetry, while the second factor enforces the glide-only constraint.

In constrast to a strongly interacting disclination Lagrangian (28) (which has no noninteracting limit), mobile dislocations admit a weakly interacting Lagrangian. Its form is constrained by the generalized global (subsystem) symmetry (33) as well as the gauge symmetry (22) and is uniquely given by (Kumar and Potter, 2019; Pretko, Zhai, and Radzihovsky, 2019)

$$\mathcal{L}_d = \sum_{\mathbf{d}} i\psi^*_{\mathbf{d}}(\partial_0 - iA_0)\psi_{\mathbf{d}} - \frac{P^{ij}_\perp}{2m}(\partial_i + id_kA_{ik})\psi^*_{\mathbf{d}}(\partial_j - id_lA_{jl})\psi_{\mathbf{d}} + V(|\psi_{\mathbf{d}}|^2), \tag{34}$$

where $P^{ij}_\perp = \delta^{ij} - d^id^j/|d|^2$ is the projector onto the axis perpendicular to the dipole moment $\mathbf{d}$ (i.e., along the Burgers vector $\mathbf{b}=\hat{\mathbf{z}}\times\mathbf{d}$), thus enforcing the glide-only constraint dictated by Eq. (33). The dipole moment enters as the "charge" of the field ψ_d under the tensor gauge field A_{ij}. The Lagrangian (34) is also invariant under discrete transformations that permute primitive lattice vectors, corresponding to the point group symmetry of the crystal.

4. Coupled-vector gauge theory duality

A complementary, more convenient, and more transparent formulation of a crystal's dual gauge theory is that given in terms of the coupled U(1) vector gauge fields that were introduced and discussed by Radzihovsky and Hermele (2020). The idea is in fact simple and is based on the observation that elasticity formulated in terms of the unsymmetrized strain $\partial_i u_k$ has a form of two flavored u_x and u_y XY models. Independent XY models would dualize to conventional nonfractonic U(1) vector gauge theories. Thus, it is the nontrivial "flavor-space" phonon coupling (a symmetrization of $\partial_i u_k$ in the conventional formulation) that is responsible for the appearance of fractons (Radzihovsky and Hermele, 2020; Qi, Radzihovsky, and Hermele, 2021). Some formal aspects of the duality were also discussed by Caddeo, Hoyos, and Musso (2022).

To get to an equivalent flavored vector gauge theory description, we reformulate the conventional elastic theory (18) in terms of minimally coupled quantum XY models by introducing the orientational bond-angle field θ and its

[9]More precisely, J^{ij} transforms in a spin-2 irreducible representation of SO(2).

canonically conjugate angular momentum density L. The Lagrangian density (characterizing the elastic constant tensor C_{ijkl} as a single elastic constant C for simplicity) is given by

$$\mathcal{L} = \pi_k \partial_0 u_k + L\partial_0\theta - \tfrac{1}{2}\pi_k^2 - \tfrac{1}{2}C(\partial_i u_k - \theta\epsilon_{ik})^2 - \tfrac{1}{2}L^2 - \tfrac{1}{2}K(\boldsymbol{\nabla}\theta)^2. \tag{35}$$

Coupling of the unsymmetrized strain $\partial_i u_k$ to $\theta\epsilon_{ik}$ "Higgses" its antisymmetric part below a scale set by C, reducing $\mathcal{L}$ to standard crystal elasticity in terms of the symmetrized strain u_{ik} [Eq. (18)], which is the starting point used by Pretko and Radzihovsky (2018a). This reformulates 2D elasticity in terms of two translational XY models for two phonons u_k coupled using the orientational XY model for the orientational bond field θ. To dualize $\mathcal{L}$, we decouple the elastic and orientational energies in Eq. (35) via Hubbard-Stratonovich vector fields, stress $\boldsymbol{\sigma}_k$ (with flavor index k inherited from $\boldsymbol{\nabla}u_k$), and torque $\boldsymbol{\tau}$. We then introduce disclinations $\boldsymbol{\nabla}\times\boldsymbol{\nabla}\theta^s = (2\pi s/n)\delta^2(\mathbf{r}) \equiv \rho(\mathbf{r})$, with charge $2\pi s/n$ ($s = \pm\mathbb{Z}$ and $n = 6$ for hexagonal crystal) and their dipoles, dislocations, and $\boldsymbol{\nabla}\times\boldsymbol{\nabla}u_k^s = b_k\delta^2(\mathbf{r}) \equiv b_k(\mathbf{r})$, with Burgers charge $\mathbf{b}$. We then integrate over the single-valued elastic components of θ and u_k. This enforces the conservation of linear and angular momenta: $\partial_0\pi_k - \boldsymbol{\nabla}\cdot\boldsymbol{\sigma}_k = 0$ and $\partial_0 L - \boldsymbol{\nabla}\cdot\boldsymbol{\tau} = \varepsilon_{ij}\sigma_{ij} \equiv \sigma_a$.

Expressing this linear momentum constraint in terms of dual magnetic and electric fields as $\pi_k = \epsilon_{kj}B_j$ and $\sigma_{ik} = -\epsilon_{ij}\epsilon_{k\ell}E_{j\ell}$ gives the k-flavored Faraday equations $\partial_0 B_k + \boldsymbol{\nabla}\times\mathbf{E}_k = 0$, which are solved using the k-flavored vector $\mathbf{A}_k$ and scalar A_{0k} gauge potentials $B_k = \boldsymbol{\nabla}\times\mathbf{A}_k$ and $\mathbf{E}_k = -\partial_0\mathbf{A}_k - \boldsymbol{\nabla}A_{0k}$. We emphasize that, in contrast to the symmetric tensor approach (Pretko and Radzihovsky, 2018a, 2018b), here the $k = (x, y)$–flavored vector gauge field $\mathbf{A}_k$ has components A_{ik} that form an unsymmetrized tensor field.

The conservation of angular momentum can now be solved with another set of vector $\mathbf{a}$ and scalar a_0 gauge fields

$$L = \boldsymbol{\nabla}\times\mathbf{a} + A_a, \qquad \tau_k = \epsilon_{kj}(\partial_0 a_j + \partial_j a_0 - A_{0j}), \tag{36}$$

leading to the dual Lagrangian density

$$\tilde{\mathcal{L}}_{\rm cr} = \tfrac{1}{2}C^{-1}(\partial_0\mathbf{A}_k + \boldsymbol{\nabla}A_{0k})^2 - \tfrac{1}{2}(\boldsymbol{\nabla}\times\mathbf{A}_k)^2 + \tfrac{1}{2}K^{-1}(\partial_0 a_k + \partial_k a_0 - A_{0k})^2 - \tfrac{1}{2}(\boldsymbol{\nabla}\times\mathbf{a} + A_a)^2 + \mathbf{A}_k\cdot\mathbf{J}_k - A_{0k}p_k + \mathbf{a}\cdot\mathbf{j} - a_0\rho, \tag{37}$$

where the dipole charge p_k is given by the dislocation density $p_k = (\hat{\mathbf{z}}\times\mathbf{b})_k$, the fracton charge ρ is the disclination density, and the corresponding currents are given by $\mathbf{J}_k = \epsilon_{lk}\hat{\mathbf{z}}\times(\partial_0\boldsymbol{\nabla}u_l - \boldsymbol{\nabla}\partial_0 u_l)$ and $\mathbf{j} = \hat{\mathbf{z}}\times(\partial_0\boldsymbol{\nabla}\theta - \boldsymbol{\nabla}\partial_0\theta)$.

The corresponding Hamiltonian density

$$\tilde{\mathcal{H}}_{\rm cr} = \tfrac{1}{2}C|\mathbf{E}_k|^2 + \tfrac{1}{2}(\boldsymbol{\nabla}\times\mathbf{A}_k)^2 + \tfrac{1}{2}K|\mathbf{e}|^2 + \tfrac{1}{2}(\boldsymbol{\nabla}\times\mathbf{a} + A_a)^2 - \mathbf{A}_k\cdot\mathbf{J}_k - \mathbf{a}\cdot\mathbf{j} \tag{38}$$

involves three U(1) vector gauge fields with electric fields $\mathbf{E}_k$ (flavors $k = x$ and y) and $\mathbf{e}$, and corresponding canonically conjugate vector potentials $\mathbf{A}_k$ and $\mathbf{a}$, with the former gauging the latter through a 2-form $A_a = \epsilon_{ik}A_{ik}$ minimal coupling $(da - A)^2$. This translational and orientational gauge field coupling encodes a semidirect product of spatial translations and rotations constrained by the generalized gauge invariance (Radzihovsky and Hermele, 2020).

The Hamiltonian is supplemented by Gauss's laws,

$$\boldsymbol{\nabla}\cdot\mathbf{E}_k = p_k - e_k, \qquad \boldsymbol{\nabla}\cdot\mathbf{e} = \rho. \tag{39}$$

Note that the components of the electric field e_k (which would be generated by the motion of charges ρ) function as an additional dipole charge in the dipole Gauss law for $\mathbf{E}_k$ [Eq. (39)], and its conservation thus encodes the fractonic immobility of the disclination charges ρ. Equivalently we note that the continuity equation for dipole densities p_k,

$$\partial_0 p_k + \boldsymbol{\nabla}\cdot\mathbf{J}_k = \mathbf{j}, \qquad \partial_0\rho + \boldsymbol{\nabla}\cdot\mathbf{j} = 0, \tag{40}$$

is violated by the charge current $\mathbf{j}$, which thus must vanish in the absence of dipole charges, i.e., $p_k = 0 \to j_k = 0$, leading to immobility of the fractonic charges enforced by gauge invariance.

Although the aforementioned elasticity-gauge duality works only in $(2+1)$D dimensions, the generalization of the gauge dual to d dimensions is straightforward (although it does not correspond to any physical elasticity) and consists of $d+1$ U(1) gauge fields obeying the same Gauss laws but with $k = 1, \ldots, d$. The main difference in the Hamiltonian is that $(\boldsymbol{\nabla}\times\mathbf{a} + A_a)^2$ is replaced by a sum of the $d(d-1)/2$ terms of the 2-form minimal coupling $(\partial_i a_j - \partial_j a_i + A_{ij} - A_{ji})^2 = (da - A)^2$. At low energies this coupled U(1) vector gauge theory reduces to the d-dimensional scalar-charge tensor gauge theory (Radzihovsky and Hermele, 2020).

C. Fracton-disclination duality: Smectic

A smectic state of matter characterized by a uniaxial spontaneous breaking of rotational and translational symmetries is ubiquitous in classical liquid crystals of highly anisotropic molecules (such as classic 4′-octyl-4-biphenylcarbonitrile) (De Gennes and Prost, 1993). Its quantum realizations range from "striped" states of a two-dimensional electron gas at half-filled high Landau levels (Koulakov, Fogler, and Shklovskii, 1996; Moessner and Chalker, 1996; Fradkin and Kivelson, 1999; Lilly *et al.*, 1999; MacDonald and Fisher, 2000; Barci *et al.*, 2002; Radzihovsky and Dorsey, 2002; Schreiber and Csáthy, 2020), striped spin and charge states of weakly doped correlated quantum magnets (Tranquada *et al.*, 1997; Kivelson, Fradkin, and Emery, 1998) of the putative Fulde-Ferrell-Larkin-Ovchinnikov paired superfluids (Fulde and Ferrell, 1964; Larkin and Ovchinnikov, 1965) in imbalanced degenerate atomic gases (Radzihovsky and Vishwanath, 2009; Radzihovsky, 2011), ferromagnetic transitions in one-dimensional spin-orbit-coupled metals (Kozii *et al.*, 2017), spin-orbit-coupled Bose condensates (Radzihovsky and Choi, 2009; Zhai, 2015), and helical states of bosons or spins on a frustrated lattice (Hsieh, Ma, and Radzihovsky, 2022). We thus next review a smectic dual gauge theory representation

and the associated quantum melting transitions from surrounding crystal and nematic phases.

The simplest description of a $(2+1)$D quantum smectic (Radzihovsky, 2020; Zhai and Radzihovsky, 2021) is in terms of a single phonon Goldstone mode with a Lagrangian density,

$$\mathcal{L}_{\rm sm} = \frac{1}{2}(\partial_0 u)^2 - \frac{\kappa}{2}(\partial_y u)^2 - \frac{K}{2}(\partial_x^2 u)^2, \tag{41}$$

which is a close cousin of the quantum Lifshitz model[10] (Ardonne, Fendley, and Fradkin, 2004; Fradkin *et al.*, 2004; Vishwanath, Balents, and Senthil, 2004; Zhai and Radzihovsky, 2019; Gorantla *et al.*, 2022; Kapustin and Spodyneiko, 2022; Lake, Hermele, and Senthil, 2022; Lake *et al.*, 2022; Radzihovsky, 2022; Zechmann *et al.*, 2022).

This more familiar low-energy universal description naturally emerges from a more "microscopic" (low-energy equivalent) formulation in terms of a phonon (layer displacement) $\mathbf{u} = u(\mathbf{r})\hat{\mathbf{y}}$ and the unit-normal (layer orientation) $\hat{\mathbf{n}}(\mathbf{r}) = -\hat{\mathbf{x}}\sin\hat{\theta} + \hat{\mathbf{y}}\cos\hat{\theta} \equiv \hat{\mathbf{y}} + \delta\hat{\mathbf{n}}$ field operators and the corresponding canonically conjugate linear and angular momentum fields $\pi(\mathbf{r})$ and $L(\mathbf{r})$, with the Hamiltonian density

$$\mathcal{H}_{\rm sm} = \tfrac{1}{2}\pi^2 + \tfrac{1}{2}L^2 + \tfrac{1}{2}\kappa(\boldsymbol{\nabla}u + \delta\hat{\mathbf{n}})^2 + \tfrac{1}{2}K(\boldsymbol{\nabla}\hat{\mathbf{n}})^2, \tag{42}$$

where κ and K are elastic constants.

Working in a phase-space path-integral formulation, the corresponding Lagrangian density is

$$\mathcal{L}_{\rm sm} = \pi\partial_0 u + L\partial_0\theta - \tfrac{1}{2}\pi^2 - \tfrac{1}{2}L^2 + \tfrac{1}{2}\kappa^{-1}\boldsymbol{\sigma}^2 + \tfrac{1}{2}K^{-1}\tau^2 - \boldsymbol{\sigma}\cdot(\boldsymbol{\nabla}u - \hat{\mathbf{x}}\theta) - \boldsymbol{\tau}\cdot\boldsymbol{\nabla}\theta. \tag{43}$$

In Eq. (43), we neglected θ nonlinearities, took the x axis to be along the smectic layers and, as with a crystal duality of Sec. III.B.4, for later convenience introduced the Hubbard-Stratonovich fields $\boldsymbol{\sigma}$ and $\boldsymbol{\tau}$ corresponding to the local stress and torque, respectively. Integrating over the auxiliary fields π, L, $\boldsymbol{\sigma}$, and $\boldsymbol{\tau}$ easily recovers the phonon-only Lagrangian in Eq. (41).

Equation (43) allows us to separate Goldstone modes into smooth and singular (defect) components and to functionally integrate over the smooth, single-valued parts of the phonon u and orientation θ fields. With this, we obtain the coupled linear and angular momenta conservation constraints

$$\partial_0\pi - \boldsymbol{\nabla}\cdot\boldsymbol{\sigma} = 0, \qquad \partial_0 L - \boldsymbol{\nabla}\cdot\boldsymbol{\tau} = \hat{\mathbf{x}}\cdot\boldsymbol{\sigma}. \tag{44}$$

[10]A generalized m Lifshitz model has an elasticity with m "soft" (Laplacian) axes and d-m complementary "hard" (gradient) axes. In this nomenclature, the conventional classical 3D smectic is the $m = 2$ Lifshitz model, and the $(2+1)$D quantum smectic and 3D classical columnar liquid crystal are described by the $m = 1$ Lifshitz model. Other generalizations include a nonscalar Goldstone mode field as in tethered membranes (Radzihovsky and Toner, 1995, 1998; Le Doussal and Radzihovsky, 2018) and nematic elastomers (Xing and Radzihovsky, 2003, 2008).

Solving these in terms of gauge fields,

$$\pi = \hat{\mathbf{z}}\cdot(\boldsymbol{\nabla}\times\mathbf{A}), \qquad \boldsymbol{\sigma} = \hat{\mathbf{z}}\times(\partial_0\mathbf{A} + \boldsymbol{\nabla}A_0),$$
$$L = \hat{\mathbf{z}}\cdot(\boldsymbol{\nabla}\times\mathbf{a} - \hat{\mathbf{x}}\times\mathbf{A}), \qquad \boldsymbol{\tau} = \hat{\mathbf{z}}\times(\partial_0\mathbf{a} + \boldsymbol{\nabla}a_0 - \hat{\mathbf{x}}A_0), \tag{45}$$

allows us to express smectic's Lagrangian density in terms of these Goldstone-mode-encoding gauge fields and to obtain the Maxwell part of the smectic dual Lagrangian,

$$\tilde{\mathcal{L}}^{\rm sm}_{\rm M} = \frac{1}{2\kappa}(\partial_0\mathbf{A} + \boldsymbol{\nabla}A_0)^2 - \frac{1}{2}(\boldsymbol{\nabla}\times\mathbf{A})^2 + \frac{1}{2K}(\partial_0\mathbf{a} + \boldsymbol{\nabla}a_0 - A_0\hat{\mathbf{x}})^2 - \frac{1}{2}(\boldsymbol{\nabla}\times\mathbf{a} - \hat{\mathbf{x}}\times\mathbf{A})^2. \tag{46}$$

As with the crystal's gauge dual in Sec. III.B.4, the smectic's gauge dual displays a nontrivial "minimal" coupling between the translational and orientational gauge fields and exhibits a generalized gauge invariance under transformations,

$$(A_0, \mathbf{A}) \to A'_\mu = (A_0 - \partial_0\phi, \mathbf{A} + \boldsymbol{\nabla}\phi), \tag{47a}$$

$$(a_0, \mathbf{a}) \to a'_\mu = (a_0 - \partial_0\chi, \mathbf{a} + \boldsymbol{\nabla}\chi - \hat{\mathbf{x}}\phi). \tag{47b}$$

The six gauge field degrees of freedom A_μ and a_μ reduce to two physical Goldstone modes after gauge fixing ϕ, χ and implementing two Gauss law constraints [Eq. (51)].

To include dislocations and disclinations, we allow for the nonsingle-valued components of u and θ, respectively, which are defined by

$$p = \hat{\mathbf{z}}\cdot\boldsymbol{\nabla}\times\boldsymbol{\nabla}u, \qquad \mathbf{J} = \hat{\mathbf{z}}\times(\boldsymbol{\nabla}\partial_0 u - \partial_0\boldsymbol{\nabla}u), \tag{48a}$$

$$\rho = \hat{\mathbf{z}}\cdot\boldsymbol{\nabla}\times\boldsymbol{\nabla}\theta, \qquad \mathbf{j} = \hat{\mathbf{z}}\times(\boldsymbol{\nabla}\partial_0\theta - \partial_0\boldsymbol{\nabla}\theta). \tag{48b}$$

Equations (48) together with $\tilde{\mathcal{L}}^{\rm sm}_{\rm M}(A_\mu, a_\mu)$ give the dual Lagrangian density for the quantum smectic

$$\tilde{\mathcal{L}}_{\rm sm} = \tilde{\mathcal{L}}^{\rm sm}_{\rm M}(A_\mu, a_\mu) + \mathbf{A}\cdot\mathbf{J} - A_0 p + \mathbf{a}\cdot\mathbf{j} - a_0\rho \tag{49}$$

corresponding to the Hamiltonian density

$$\tilde{\mathcal{H}}_{\rm sm} = \tfrac{1}{2}\kappa\mathbf{E}^2 + \tfrac{1}{2}(\boldsymbol{\nabla}\times\mathbf{A})^2 + \tfrac{1}{2}K\mathbf{e}^2 + \tfrac{1}{2}(\boldsymbol{\nabla}\times\mathbf{a} - \hat{\mathbf{x}}\times\mathbf{A})^2 - \mathbf{A}\cdot\mathbf{J} - \mathbf{a}\cdot\mathbf{j}. \tag{50}$$

Equation (50) supplemented by the generalized Gauss law constraints,

$$\boldsymbol{\nabla}\cdot\mathbf{E} = p - \mathbf{e}\cdot\hat{\mathbf{x}}, \qquad \boldsymbol{\nabla}\cdot\mathbf{e} = \rho. \tag{51}$$

p and $\mathbf{J}$ are $\hat{\mathbf{x}}$ dipole charge and current densities representing $\hat{\mathbf{y}}$ dislocations, while ρ and $\mathbf{j}$ are fractonic charge and current densities corresponding to disclinations. The generalized gauge invariance of Eq. (50) imposes coupled continuity equations for the densities

$$\partial_0 p + \boldsymbol{\nabla}\cdot\mathbf{J} = -\mathbf{j}\cdot\hat{\mathbf{x}}, \qquad \partial_0\rho + \boldsymbol{\nabla}\cdot\mathbf{j} = 0, \tag{52}$$

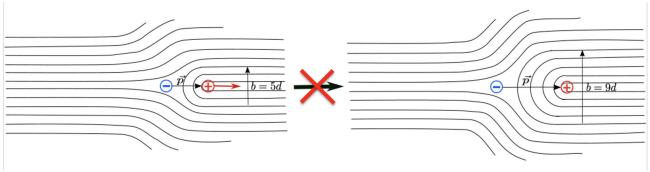

FIG. 6. Illustration of restricted along-layers mobility of $+/-$ disclination (lineon) charges (making up a dislocaton b, i.e., a dipole p) in a quantum smectic, forbidding their separation, which corresponds to a nonlocal process of adding a smectic half layer per lattice constant of charge separation.

where dipole conservation is violated by a nonzero charge current $\mathbf{j}\cdot\hat{\mathbf{x}}$ along smectic layers.

Equations (52) thus transparently encode the restricted mobility of the disclination charges ρ, illustrated in Fig. 6, with a relaxation rate $\Gamma_k = Dk_y^2 + \gamma k_x^4$, resulting in slow subdiffusive decay $\rho(t) \sim 1/t^{3/4}$, and mobility and diffusion coefficients vanishing along the $\hat{\mathbf{x}}$-directed smectic layers, i.e., $\mathbf{j}\cdot\hat{\mathbf{x}} = 0$ in the absence of dislocation dipoles (Feldmeier *et al.*, 2020; Gromov, Lucas, and Nandkishore, 2020; Guardado-Sanchez *et al.*, 2020; Radzihovsky, 2020; Glorioso *et al.*, 2022; Guo, Glorioso, and Lucas, 2022).

D. Quantum melting

Starting with the gauge dual of the quantum crystal (derived in Sec. III.B.1), either in tensor (34) or in its equivalent coupled-vector gauge theory form (37), and minimally coupling it to dynamic dislocation-dipole matter (ψ_d) gives a quantum Lagrangian density,

$$\tilde{\mathcal{L}}_{\rm cr} = \sum_{k=1,2}\frac{J_k}{2}|(\partial_\mu - iA_\mu^k)\psi_k|^2 - V(\{\psi_k\}) + \mathcal{L}_{\rm M}^{\rm cr}(A_{1,\mu}, A_{2,\mu}, a_\mu), \tag{53}$$

where $\psi_{k=1,2}$ correspond to $\hat{\mathbf{p}}_{1,2}$ dipoles (two elementary dislocations), $A_{k,\mu}$, a_μ gauge fields capture the kth phonons and bond orientational Goldstone modes (with unit dipole charges p_k absorbed into the definitions of $A_{k,\mu}$), and $V(\psi_1,\psi_2)$ is a U(1)-symmetric Landau potential, with a dual Maxwell Lagrangian (37). This field theory[11] thus gives a complete description of the quantum melting transitions out of the fractonic crystal state. The nature of this quantum transition is then dictated by the form of the dipole interaction potential $V(\psi_1,\psi_2)$.

1. Crystal-to-hexatic Higgs transition

In a 2D hexagonal (square) crystal, the C_6 (C_4) invariance enforces the symmetry between ψ_1- and ψ_2-dislocation dipoles; i.e., their interaction potential $V(\psi_1,\psi_2)$ is $1\leftrightarrow 2$ symmetric. Thus, as illustrated in Fig. 7, driven by quantum

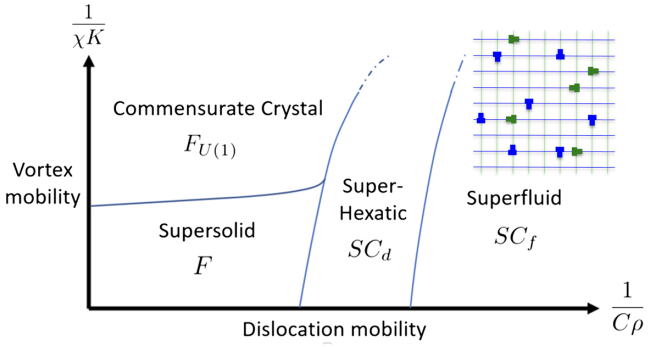

FIG. 7. Schematic illustrating phases derived from the supersolid [a U(1)-symmetry-broken fracton phase F]. Upon condensation of vortex defects, bosons can transition to a commensurate-crystal [a U(1)-symmetric fracton phase $F_{\rm U(1)}$], superhexatic, or superfluid phase. Note that U(1)-symmetric liquid and hexatic phases are forbidden at zero temperature for reasons summarized in Fig. 12.

fluctuations both types of dipoles unbind and Bose condense at a single Higgs transition, that is, the quantum crystal-to-hexatic (tetratic) melting, the counterpart of the well-known 2D classical thermal melting transition predicted by Kosterlitz and Thouless, Halperin and Nelson, and Young (Kosterlitz and Thouless, 1973; Halperin and Nelson, 1978; Young, 1979; Zhai and Radzihovsky, 2019).[12] The Higgs transition thus gaps out both translational gauge fields $A_{1,\mu}$ and $A_{2,\mu}$, which can therefore be safely integrated out, or to lowest order effectively set to zero. This reduces the coupled gauge theory to a conventional Maxwell form for the remaining rotational gauge field a_μ, with

$$\mathcal{L}_{\rm M}^{\rm hex}(a_\mu) \approx \mathcal{L}_{\rm M}^{\rm cr}(A_{1,2\mu}\approx 0, a_\mu) = \tfrac{1}{2}K^{-1}\mathbf{e}^2 - \tfrac{1}{2}(\boldsymbol{\nabla}\times\mathbf{a})^2. \tag{54}$$

As expected, it is the dual to the quantum XY model of the orientationally ordered quantum hexatic (tetratic) liquid[13] $\mathcal{L}_{\rm hex} = (1/2)(\partial_0\theta)^2 - (1/2)K(\boldsymbol{\nabla}\theta)^2$. As with the conventional U(1) Higgs (normal-superconductor) transition, the mean-field approximation breaks down for $d+1\le 4$ and may be driven to first order by translational gauge field $A_{k,\mu}$ fluctuations (Halperin, Lubensky, and Ma, 1974; Radzihovsky, 1995). Analysis of the non-mean-field criticality of this quantum crystal-superhexatic (supertetratic) melting transition remains an open problem.

2. Crystal-to-smectic Higgs transition

An alternative to the aforementioned direct, continuous crystal-to-hexatic (or crystal-to-tetratic) quantum melting scenario is a two-stage transition that takes place in a uniaxial

[11] As discussed in Sec. III.D.1, for a complete description it must be supplemented by the vacancy and interstitial (atom) sector captured by a conventional Abelian-Higgs model with bosonic matter.

[12] A classical electrostatic limit of the crystal's gauge dual reduces Eq. (53) to a vector sine-Gordon model $\tilde{H} = (1/2)\tilde{C}^{-1}_{ij,kl}\partial_i\partial_j\phi\partial_k\partial_l\phi - g_b\sum_{n=1}^{p}\cos(\mathbf{b}_n\cdot\hat{z}\times\nabla\phi) - g_s\cos(s_p\phi)$ that reproduces (Zhai and Radzihovsky, 2019) the two-stage crystal-hexatic-isotropic melting of the Kosterlitz-Thouless-Halperin-Nelson-Young model.

[13] Because a condensation of dislocations necessarily leads to Bose condensation of bosonic vacancies and interstitials, the resulting hexatic fluid is necessarily a superfluid, i.e., a superhexatic.

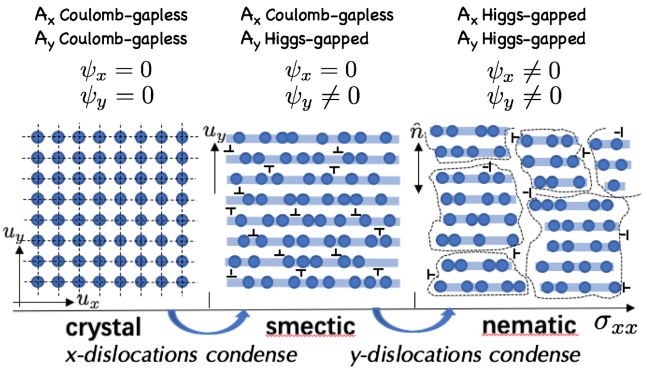

FIG. 8. Illustration of quantum melting of a 2D crystal into a smectic melting followed by a smectic-to-nematic melting, driven, respectively, by condensations of b_x (ψ_y dipoles) and b_y (ψ_x dipoles) dislocations.

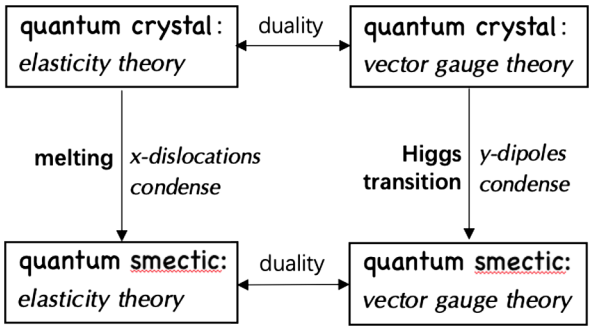

FIG. 9. Quantum crystal-smectic duality relations and the associated quantum melting transition.

crystal where C_6 or C_4 symmetry is broken down to C_2, as illustrated in Fig. 8. The reduced uniaxial symmetry is necessarily encoded in the Landau potential $V(\psi_1, \psi_2)$, specifically, controlled by the quadratic term $g_k|\psi_k|^2$, with $g_2 < g_1$ leading to a condensation of ψ_2-dislocation dipoles, with ψ_1 remaining gapped.

Alternatively, this breaking of C_6 (or C_4) symmetry down to C_2 may happen spontaneously, with $g_1 = g_2$ instead controlled by the sign of the v coupling in the dislocation interaction $v|\psi_x|^2|\psi_y|^2$. For $v > 0$, only one of the two dipole species condenses, say, $\psi_2 \neq 0$ with $\psi_1 = 0$. This Higgs transition thus only gaps out $A_{2,\mu}$, which then can be safely integrated out. To lowest order this corresponds to $A_{2\mu} \approx 0$, thereby reducing the crystal's Maxwell Lagrangian to that of the quantum smectic (41), with

$$\mathcal{L}_{\rm M}^{\rm sm}(A_{1,\mu}, a_\mu) \approx \mathcal{L}_{\rm M}^{\rm cr}(A_{1,\mu}, A_{2,\mu} \approx 0, a_\mu). \tag{55}$$

While this phase transition faithfully captures the crystal-smectic melting at the mean-field level, as with the crystal-hexatic Higgs transition, its true critical properties are expected to be nontrivial and remain to be analyzed. The two ways of obtaining the smectic gauge dual (by dualizing a smectic Lagrangian and through the aforementioned Higgs melting transition of the crystal's gauge dual) are summarized in Fig. 9.

3. Quantum smectic-to-nematic Higgs transition

As illustrated in Fig. 8, the aforementioned crystal-to-smectic transition is then naturally followed by quantum melting into a nematic superfluid by condensation of ψ_1 dipoles (aligned with the smectic layers), i.e., a proliferation of $\mathbf{b}_1$ dislocations with Burgers vectors transverse to smectic layers. The resulting $\psi_1 \neq 0$ Higgs phase gaps out the remaining smectic translational gauge field $A_\mu (= A_\mu^x)$, which can therefore be safely integrated out. This reduces the model to a conventional Maxwell form for the rotational gauge field a_μ, with

$$\mathcal{L}_{\rm M}^{\rm nem}(a_\mu) \approx \mathcal{L}_{\rm M}^{\rm sm}(A_\mu \approx 0, a_\mu) = \tfrac{1}{2}K^{-1}\mathbf{e}^2 - \tfrac{1}{2}(\boldsymbol{\nabla} \times \mathbf{a})^2, \tag{56}$$

that is, a dual to the quantum XY model of the nematic $\mathcal{L}_{\rm nem} = (1/2)(\partial_0\theta)^2 - (1/2)K(\boldsymbol{\nabla}\theta)^2$. Fluctuation corrections lead to an anisotropic stiffness and subdominant higher-order gradients. As with the conventional U(1) Higgs normal-superconductor transition, a mean-field approximation breaks down for $d + 1 \leq 4$, and may be driven to first order by fluctuations of the translational gauge field A_μ (Halperin, Lubensky, and Ma, 1974; Radzihovsky, 1995). An analysis of the non-mean-field criticality of the quantum smectic-nematic transition also remains an open problem.

E. Supersolid, superhexatic, supersmectic: Vacancies and interstitials

As discussed in Sec. III.B.1, thus far we have neglected vacancies and interstitials (see Fig. 10), which physically correspond to a restriction to their Mott-insulating, commensurate-crystal state. This misses the additional atomic sector of the system encoded by a Bose-Hubbard (quantum XY) model or its gauge-dual Abelian-Higgs model from Sec. III.A. The need for this missing vacancy and interstitial (atomic) sector is clear, as quantum melting a crystal of bosons at zero temperature and in the absence of a substrate or disorder generically leads to a gapless superfluid.

Thus, as discussed by Pretko and Radzihovsky (2018b), Kumar and Potter (2019), and Pretko, Zhai, and Radzihovsky (2019) and illustrated in Fig. 7, at zero temperature two qualitatively distinct commensurate and incommensurate quantum crystals are possible, distinguished as the Mott-insulating and superfluid states of this atomic vacancy and interstitial sector, respectively. In the former, the U(1)

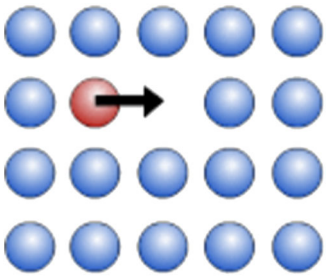

FIG. 10. Mobile vacancy and interstitial defects of a crystal, which are necessary to faithfully capture the associated supersolid and superfluid phases.

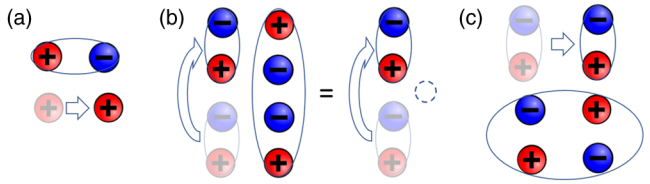

FIG. 11. (a) Fracton motion is forbidden, as it requires emission of a conserved dipole. (b) In the $F_{\mathrm{U}(1)}$-charge-enriched fractonic phase (commensurate-crystal) longitudinal dipole motion (dislocation climb) is forbidden, as it requires the emission of a linear quadrupole carrying conserved vacancy or interstitial number corresponding to local compression of the crystal, i.e., a vacancy defect. (c) Transverse dipole motion (dislocation glide) is allowed, as it creates a square quadrupole corresponding to a local shear.

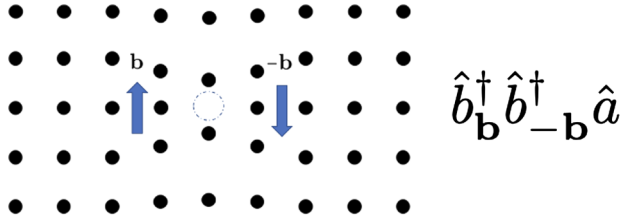

FIG. 12. Constructed as a bound state of two equal and opposite dislocations with Burgers vectors $\mathbf{b}$ and $-\mathbf{b}$, a disclination quadrupole carrying a unit of vacancy (atom) number, a local defect that can be seen as a deficiency of an atom in the middle of the configuration, as illustrated in Fig. 10. This construction demonstrates the allowed $\hat{b}^\dagger{}_{\mathbf{b}}\hat{b}^\dagger_{\mathbf{b}}\hat{a}$ operator, which is encoded such that the condensation of dipoles is necessarily accompanied by the condensation of vacancies and intetstitials and thus leads to superfluidity of the fluid phases.

symmetry-enriching constraint imposes a glide-only motion of dislocation (illustrated in Figs. 5 and 11) that is broken in the latter, where the dipole dislocation motion is unconstrained (Marchetti and Radzihovsky, 1999; Pretko and Radzihovsky, 2018b).

Under duality, these two types of quantum crystals then map onto two distinct fractonic phases $F_{U(1)}$ and F, respectively, with and without quadrupole-imposed restriction on the dipole glide-only and unrestricted motion, as illustrated in Figs. 11(b) and 11(c) (Pretko and Radzihovsky, 2018b).

This dipole constrained motion condition is concisely encoded in the Ampère law of the corresponding tensor gauge theory,

$$\partial_0 E^{ij} + \tfrac{1}{2}(\epsilon^{ik}\partial_k B^j + \epsilon^{jk}\partial_k B^i) = -J^{ij}, \tag{57}$$

whose trace can be expressed in terms of the vacancy-interstitial density $n_d = E^i_i + n_0\partial_i u_i$ and the corresponding current $J^i_d = \pi^i$,

$$\partial_0 n_d + \partial_i \pi^i = -J^i{}_i, \tag{58}$$

where we used $E^i{}_i = n_d - n_0\partial_i u_i \approx n_d$, which was first derived by Marchetti and Radzihovsky (1999). With this vacancy-interstitial continuity equation [sourced by $J^i{}_i$, corresponding to the longitudinal (along-dipole) motion of dipoles (Pretko, 2017b; Pretko and Radzihovsky, 2018b)], Eq. (58) is encoded such that the climb of dislocations creates vacancy-interstitial defects. Conversely, the Mott-insulating (commensurate-crystal) state of the latter restricts the motion of dislocations to glide-only lineon type, dualizing to a symmetry-enriched fracton state $F_{\mathrm{U}(1)}$. It can then undergo a quantum phase transition to a distinct fracton state F when vacancies and interstitials Bose condense, thereby breaking the atom-number $\mathrm{U}(1)$ symmetry. The corresponding phase diagram is illustrated in Fig. 7.

In contrast to a crystal that allows an $F_{\mathrm{U}(1)}$ ground state, we observe that hexatic and smectic states are dislocation condensates [corresponding to the condensation of both or just one of the $\hat{\mathbf{x}}$- and $\hat{\mathbf{y}}$-dislocation dipoles (created by $\hat{b}^\dagger_{\mathbf{b}}$)]. Thus, vacancies and interstitials (created by $\hat{a}^\dagger$ and illustrated in Fig. 12) consisting of pairs of oppositely charged dislocations (disclination charge quadrupoles) are necessarily driven to Bose condense by the allowed coupling $\hat{a}\hat{b}^\dagger_{\mathbf{b}}\hat{b}^\dagger_{-\mathbf{b}}$. Thus, a hexatic and a smectic are necessarily incommensurate "superhexatic" and "supersmectic," respectively, and their dual gauge theory (50) is implicitly understood to be coupled (via axionlike $\mathcal{E}$-B and $\mathcal{B}$-E couplings) to a conventional $\mathrm{U}(1)$ gauge theory with fields $\mathcal{E}$ and B, a dual to the liquid of vacancies and interstitials (Pretko and Radzihovsky, 2018b; Pretko, Zhai, and Radzihovsky, 2019).

F. External perturbations

With an eye toward experimental probes, we now discuss the role of external perturbations. A crystal's analog of a chemical potential is the imposed velocity, a "momentum chemical potential" that imposes a nonzero density of finite-momentum boson density $n_{\mathbf{G}}$, i.e., a nonzero momentum on the crystal. On the dual side this corresponds to an external dual-magnetic field. In the dual-nonsuperconducting state of vanishing disclination and dislocation density, the response is linear, as expected due to a crystal's Galilean invariance. In contrast, the dual superconductor expels the imposed flux, either completely in a dual-Meissner state or in a "mixed" Abrikosov-like state, respectively, corresponding to a viscous response of a fluid or as a lattice of dislocations carrying a nonzero momentum.

A crystal can also be subjected to a compressive or shear stress that on the dual side is an imposition of a tensor electric field. A dislocation will generically be set in motion by the associated Peach-Koehler force $E_{ij}p_j$ encoded as an imposed dual electrictrostatic field on a charged dipole particle p_j. In the absence of dipoles this probes the response of the external tensor field across the dual "dielectric." For stress above a critical value, a dual dielectric breakdown corresponding to a proliferation of dipole dislocations will take place. The response of a smectic is more complex: it is dual Meissner-like along and nonsuperconducting across the smectic layers.

A substrate also plays a qualitatively interesting role, as it breaks the underlying rotational and translational symmetries, thereby breaking angular and linear momentum conservations. Repeating the duality analysis for a translationally incommensurate substrate, we find that it reduces the

orientational U(1) sector $(\mathbf{e}, \mathbf{a})$ to a discrete Z_n gauge theory (for n-fold orientational commensurability) coupled to a noncompact U(1) translational-sector gauge theory $(\mathbf{E}_k, \mathbf{A}_k)$. For $n = 1$ *à la* Polyakov confinement in $(2+1)$D, the orientational degrees are eliminated and the translational sector reduces to two conventional decoupled U(1) gauge theories, for $k = x$ and y. These are compact in the presence of a translationally p-fold commensurate substrate and will also be reduced to discrete Z_p gauge theories and are fully confined, i.e., pinned for $p = 1$.

G. Vortex crystal

The superfluid state formed after condensation of dislocations supports another type of topological defect: vortices. When vortices are induced by, for example, rotation or proliferate due to quantum or thermal fluctuations, they may form either a crystal, a liquid crystal, or a vortex fluid. We review these states from the fracton point of view in Secs. III.G and III.H.

We now consider the constrained dynamics of vortices. The first system of interest is a vortex crystal. We assume that it was formed by nucleating a large number of vortices in a superfluid. The elasticity of a vortex crystal is described in terms of both superfluid phase degree of freedom and vortex-lattice phonons. The low-energy Lagrangian takes the following form:

$$\mathcal{L} = -\frac{1}{2}\Gamma\bar{n}\epsilon^{ij}u_i\partial_0 u_j - \frac{1}{2}C_{ijkl}u_{ij}u_{kl} + \Gamma e_i u^i + \frac{1}{g^2}(e^2 - b^2), \tag{59}$$

where Γ is the vorticity, $\bar{n}$ is the superfluid density, and the dual electromagnetic fields e_i and b capture the Goldstone modes of the superfluid; see Sec. III.A. The first term (a single time derivative Berry phaselike term) in Eq. (59) is unique to the vortex crystals and explicitly breaks parity. It originates from the Magnus force (associated with a nonzero boson density that is seen by the vortices as an effective magnetic field) experienced by the vortices, encoding the noncommutativity of u_x and u_y.

The duality transformation follows the steps similar to those discussed previously, and the final dual Lagrangian is (Pretko, Zhai, and Radzihovsky, 2019; Nguyen, Gromov, and Moroz, 2020)

$$\begin{aligned}\tilde{\mathcal{L}} = &\frac{1}{2\Gamma\bar{n}}\epsilon^{ij}(B_i - \Gamma\epsilon_i{}^k a_k)\partial_0(B_j - \Gamma\epsilon_j{}^l a_l)\\ &+\tfrac{1}{2}\tilde{C}^{-1}_{ijkl}(E^{ij} + \Gamma\delta^{ij}a_0)(E^{kl} + \Gamma\delta^{kl}a_0).\end{aligned} \tag{60}$$

The tensor and vector gauge sectors are coupled through a nontrivial minimal-like coupling akin to the coupled-vector gauge theories of crystal (Sec. III.B.4) and smectic duals (Sec. III.C) (Radzihovsky and Hermele, 2020; Radzihovsky, 2020; Zhai and Radzihovsky, 2021). The gauge transformations act as follows:

$$\delta A_{ij} = \partial_i\partial_j\alpha + \Gamma\delta_{ij}, \quad \delta A_0 = -\partial_0\alpha, \quad \delta a_\mu = \partial_\mu\beta. \tag{61}$$

The first term in Eq. (60) has no analog in ordinary electromagnetism. The dipole conservation law (25) remains the same; however, the glide constraint is modified due to the possibility of vortex creation in the superfluid, akin to the earlier discussion of vacancies and interstitials in an incommensurate atomic crystal [Eq. (58)],

$$\partial_\mu j^\mu = J^{ii}, \tag{62}$$

where j^μ is the superfluid vortex current. The glide constraint (62) states that the dislocations can climb at the expense of vortex creation (i.e., they can violate the vortex continuity equation $\partial_\mu j^\mu = 0$) (Marchetti and Radzihovsky, 1999).

An analysis of vortex-lattice melting similar to the discussion in Sec. III.D was presented by Nguyen, Gromov, and Moroz (2020).

H. Vortex fluid

Notably a classical system of interacting vortices (or, equivalently, electric charges in a strong magnetic field) conserves the dipole moment on its own, and is thus fractonic. We demonstrate this in the example of a classical system of N vortices.

On increasing vortex density (such as by rotation), we expect a vortex crystal to melt into a vortex fluid. Neglecting dissipation, at zero temperature a vortex system can be approximated as a Hamiltonian for any number of vortices and is described by the following Lagrangian:

$$\mathcal{L} = 2\pi\sum_\alpha \gamma_\alpha x_1^\alpha \partial_0 x_2^\alpha - 2\pi\sum_{\alpha<\beta}\gamma_\alpha\gamma_\beta \ln|x^\alpha - x^\beta|. \tag{63}$$

We note that Eq. (63) neglects the effects of vortex drag and the normal component of a superfluid.

Owing to translational and rotation invariance, the total linear and angular momenta are conserved. However, because of the noncommutative nature of the vortex coordinates in Eq. (63) the linear momentum is equal to the dipole moment rotated by $\pi/2$ and the angular momentum coincides with the trace of the quadrupole moment,

$$P_i = \epsilon_{ij}\sum_\alpha \gamma_\alpha x_j^\alpha = \epsilon_{ij}Q_j, \quad L = \sum_\alpha \gamma_\alpha x_j^\alpha x_j^\alpha = \mathrm{tr}(Q_{ij}). \tag{64}$$

Consequently, a vortex dipole moves perpendicularly to the dipole moment, while isolated vortices are immobile (Doshi and Gromov, 2021). Exactly the same Lagrangian describes the electrons at the lowest Landau level, where these conservation laws are related to the area-preserving diffeomorphism symmetry (Gromov, 2019b; Du *et al.*, 2022).

The vortex lattice discussed in Sec. III.G can melt into a vortex liquid. This liquid can be understood as a hydrodynamic limit of Eq. (63). It retains the same conservation laws as the finite N system, and its continuity equation takes the same form as the traceless scalar-charge theory (25).

I. Geometric theory of defects

We have discussed two complementary approaches to elasticity and crystalline defects. In this section we make a connection between fractons and the geometric description of crystalline defects. This description dates back to the work of Kondo (1949) and is valid in all spatial dimensions. The disclinations and dislocations are described using Riemann-Cartan (RC) geometry, while the phonons are described by the fluctuations of the metric. The geometric theory of defects leverages RC geometry to describe physical properties of defects as well as defect-phonon scattering (Katanaev and Volovich, 1992).

The description of dislocations and disclinations in RC geometry can be understood by noting that torsion T^a_{ij} and curvature R^{ab}_{ij} (the main ingredients of the RC geometry) correspond to defects in translational and rotational symmetries. This follows directly from the definition[14]

$$[\boldsymbol{\nabla}_i, \boldsymbol{\nabla}_j] v^a = T^b_{ij} \partial_b v^a + R^a{}_{b;ij} v^b. \tag{65}$$

Equation (65) states that transporting a vector v^a around a small loop leads to an infinitesimal rotation by R^{ab} (Franck angle) and translation by T^a (Burgers vector).

The relation between dislocations and disclination dipoles is built into the structure of RC geometry and is phrased as a relation between the Levi-Civita curvature and the torsion,

$$2R = \partial_i (\epsilon^a{}_b e^i_a T^b), \tag{66}$$

where e^i_a is the frame field, $T^b = T^b_{ij} \epsilon^{ij}$, and R is the Ricci scalar curvature constructed from the curvature 2-form $R^a{}_{b;ij}$ (Nakahara, 2018). A similar relation plays a foundational role in the teleparallel formulation of gravity, in which the spacetime geometry is described using torsion (Blagojevic and Hehl, 2012). RC geometry further supplies us with a geometric formulation of Eqs. (7), (40), and (52) by virtue of the Bianchi identity. We illustrate the relationship in two spatial dimensions. It becomes physically transparent when we define the dislocation and disclination currents in terms of torsion and curvature according to

$$J^\mu_a = \epsilon^{\mu\nu\rho} T_{a,\nu\rho}, \qquad \Theta^\mu = \epsilon^{\mu\nu\rho} R_{\nu\rho}. \tag{67}$$

The Bianchi identity then takes the following form [Eq. (7)]:

$$\boldsymbol{\nabla}_\mu J^\mu_a = \epsilon_{ab} e^b_\rho \Theta^\rho. \tag{68}$$

Finally, we discuss the origins of the glide constraint in the RC language. The glide constraint requires extra information regarding the conservation of the total number of lattice sites. The latter can be formulated in an effective geometric way as follows. To begin, we introduce a current of lattice sites as follows:

$$J^\mu = \epsilon^{\mu\nu\rho} \epsilon_{ab} e^a_\nu e^b_\rho. \tag{69}$$

The conservation of the number of lattice sites then takes the form of the continuity equation

$$\partial_\mu J^\mu = 0. \tag{70}$$

The conserved quantity is the total volume, which translates to the total number of lattice sites,

$$V = \int d^2x J^0 = \int d^2x \, \det(e^a_i). \tag{71}$$

The glide constraint becomes more transparent after rewriting Eq. (70) as

$$\partial_0 \det(e^a_i) + 2 e^b_0 \epsilon_{ab} J^a_0 = 0, \tag{72}$$

where $J^a_0 = \sum_I b^a \delta(x - x_I)$ is the dislocation density defined by Eq. (67) and the temporal frame e^b_0 plays the role of the velocity field. Thus, the local volume $\det(e^a_i)$ changes when the dislocations are carried out in the direction perpendicular to the Burgers vector. Equation (70) has to be postulated, in addition to the RC structure.

J. Diverse realizations of tensor gauge theories

Since the original identification of fractons with crystals and liquid crystals (Pretko and Radzihovsky, 2018a, 2018b, 2020; Gromov, 2019b, 2020; Kumar and Potter, 2019; Pretko, Zhai, and Radzihovsky, 2019; Zhai and Radzihovsky, 2019, 2021; Gromov and Surowka, 2020; Nguyen, Gromov, and Moroz, 2020; Radzihovsky and Hermele, 2020), fractons have naturally appeared in a number of other elastic systems that support geometric defects. Again, fractons emerge after an appropriate duality transformation. Here we review a few of these interesting connections.

1. Fragile amorphous solids

A symmetric tensor gauge theory and its associated fractonic order have also been applied to amorphous fragile solids and granular media. These are highly nonequilibrium and heterogeneous solid states that can sustain external shear (O'Hern *et al.*, 2003; Behringer and Chakraborty, 2019). The effective long wavelength elasticity (Nampoothiri *et al.*, 2020) emerges from local force and torque balance constraints of mechanical equilibrium on every grain when the force chain of contacting grains percolates. In a continuum these grains can be encoded through a condition of mechanical equilibrium on the local symmetric stress tensor $\sigma_{ij}(\mathbf{r})$ and external force $f_i(\mathbf{r})$ satisfying

$$\partial_i \sigma_{ij}(\mathbf{r}) = f_j(\mathbf{r}). \tag{73}$$

As with crystalline solids this static equilibrium condition (73) can be naturally interpreted as a generalized Gauss law

$$\partial_i E_{ij}(\mathbf{r}) = \rho_j(\mathbf{r}) \tag{74}$$

[14]Here indices $a, b, c, \ldots$ refer to the tangent space, indices $\mu, \nu, \rho, \ldots$ refer to the spacetime, and indices $i, j, k, \ldots$ refer to the space.

for a vector-charge U(1) rank-2 tensor gauge theory (Pretko, 2017a), with a symmetric electric field tensor E_{ij} and the vector-charge density ρ_i describing the external force f_i (Nampoothiri *et al.*, 2020). This formulation then automatically encodes the net force and torque balance through vector-charge and dipole moment neutrality.

The amorphous solid elasticity is then postulated to be governed by the pseudoelectrostatics, with the energy density $\mathcal{H} = (1/2)C_{ijkl}E_{ij}E_{kl}$ and curl-free condition on the electric field coming from the electrostatic limit of Faraday's law. The latter implies the existence of an electrostatic potential that plays the role of an effective phononlike field that, unlike crystals, arises in the absence of spontaneous breaking of translational symmetry. The rank-4 elastic tensor C_{ijkl} is to be determined experimentally and is generically heterogeneous and anisotropic. The formulation then allows for an efficient computation of the stress-stress correlations associated with a distribution, geometry, and topology of the force-chain network via the $\langle E_{ij}E_{kl}\rangle$ correlator. The latter gives fourfold pinch-point singularities characteristic of the tensor gauge theory (Prem *et al.*, 2018; Pretko, Zhai, and Radzihovsky, 2019).

In contrast to a tensor gauge theory of crystalline solids, which as we reviewed here can be derived explicitly through duality (Pretko and Radzihovsky, 2018a), this gauge theory formulation of amorphous solids is a conjecture that requires the support of numerics and experiments. Indeed, the measured averaged stress-stress correlations are well fit by the electric field correlator of the vector-charge tensor gauge theory (Nampoothiri *et al.*, 2020). Fitting this to numerics and experiments (Geng *et al.*, 2001; Bi *et al.*, 2011) allows one to extract the average pseudodielectric tensor C_{ijkl} that fully characterizes the emergent static elasticity of the amorphous solid. The resulting tensor gauge theory can then be used to further explore the solid's phenomenology, such as its response to perturbations, melting, and dynamics.

2. Elastic sheets

Another interesting connection, developed by Manoj, Moessner, and Shenoy (2021), is the application of fractonic tensor gauge theory to thin elastic sheets and their associated defects, like folds and tears. With this they presented a tensor gauge theory view of the kirigami mechanics. The fractonic dual theory transparently encodes a number of known properties of such defects in thin sheets. They showed that the observation that folding of a sheet of paper can be done only along a straight line can be interpreted using the language of fractons and the restricted mobility of vector-charge tensor gauge theory.

Manoj, Moessner, and Shenoy (2021) formulated the sheet elasticity in terms of its out-of-plane flexural field $h(x, y)$ while (questionably) neglecting the in-plane phonon displacements $\mathbf{u}(x, y)$. This model then corresponds to a fluid rather than an elastic membrane (Nelson, Piran, and Weinberg, 1989; Le Doussal and Radzihovsky, 2018). The sheet's local momentum density $\sim\partial_0 h$ is identified with the scalar magnetic flux density B, the sheet's curvature tensor $\partial_\alpha\partial_\beta h$ is associated with the tensor electric field $E_{\alpha\beta}$, and the flexural modes are identified with a quadratically dispersing photon. A "tear" defect is characterized by a nonzero closed line integral of $\partial_\alpha h$ around the end of the defect, thereby capturing a nonquantized discontinuity Δh across a tear. This out-of-plane discontinuity ray has some formal similarity with the in-plane dislocation defect. A "fold" defect, an undeformable line along which there is a sheet's tangent vector discontinuity across the fold, is characterized by a closed line integral of $\partial_\alpha\partial_\beta h$. It maps onto a fractonic vector charge (the end point of the fold) of the tensor gauge theory. One hopes that such a formulation can be useful in the exploration of the quantum dynamics and statistical mechanics of kirigami sheets.

3. Quasiperiodic systems

Another interesting example is that of quasicrystals (QCs), whose elasticity-fracton duality was investigated by Surowka (2021). As developed by its pioneers (Levine and Steinhardt, 1984; Kalugin, Kitaev, and Levitov, 1985; Lubensky, Ramaswamy, and Toner, 1985) and discussed by Ding *et al.* 1993)), the elasticity of the QCs is characterized by two sets of low-energy modes: phonons described by the symmetric strain tensor u_{ij} and phasons described by a general rank-2 tensor w_{ij}. Consequently, the equations of motion are formulated in terms of two stress tensors T_{ij} and H_{ij}. These can be defined as derivatives of the Lagrangian density

$$T_{ij} = -\frac{\partial\mathcal{L}}{\partial u_{ij}}, \qquad H_{ij} = -\frac{\partial\mathcal{L}}{\partial w_{ij}}, \tag{75}$$

with [as evident from Eq. (75)] the stress tensor H_{ij} nonsymmetric. Duality transformation follows the steps reviewed in Sec. III.B.1. Under duality each QC stress is described by a dual tensor gauge field, with a traceless scalar-charge theory A_{ij}, A_0 for T_{ij} and the general rank-2 tensor $\mathcal{A}_{ij}, \mathcal{A}_0$ characterizing H_{ij}. In the dual gauge theory these degrees of freedom are coupled and the Lagrangian takes the Maxwell form; i.e., it is formulated as a quadratic form in terms of tensor electric and magnetic fields.

Associated with phonons and phasons, QCs exhibit two types of topological defects: those of u_{ij} (i.e., dislocations and disclinations) and defects of w_{ij} known as stacking faults (Lubensky, Ramaswamy, and Toner, 1985). Disclinations are scalar charges, while stacking faults are vector charges coupled to A_{ij}, A_0 and $\mathcal{A}_{ij}, \mathcal{A}_0$ tensor gauge fields. The mobility of the dislocations in QCs (and QC symmetry-protected topological states) was carefully studied by Else *et al.* (2021), who found that the dislocations are lineons with the mobility direction determined by the Burgers vector and additional topological information.

A particular example of a quasiperiodic system is the moiré superlattice generated in twisted bilayer graphene (Gaa *et al.*, 2021). The phasons in moiré systems correspond to a relative displacement of the layers. Singularities of the phason modes in this context were referred to as discompressions by Gaa *et al.* (2021), which were indeed found to be immobile.

IV. GLOBAL SYMMETRIES AND GAUGE THEORIES

Tensor gauge theories describe fields that naturally mediate interactions between fractons in a manner similar

to electromagnetism. They were first introduced by Kleinert (1983) in a discussion of a dual approach to the melting transition. Later lattice versions of these gauge theories took the form of low-energy effective theories of spin liquids (Xu and Horova, 2010).

We encountered such gauge theories in Sec. III as duals of elastic systems. Here we present a symmetry perspective on these theories and explain how they arise from gauging an abstract symmetry algebra: *multipole algebra*. This approach allows us to generalize tensor gauge theories to multipole gauge theories that are related to both anisotropic liquid crystals and fractal surface codes.

A. General symmetric tensor gauge theories

Tensor gauge theories such as Eq. (23) arise from gauging a global algebra of conserved charge and multipole moments. This algebra has to include spatial symmetries such as translations and rotations because they do not commute with multipole charges. The simplest case of this algebra includes all multipole charges up to some rank r and all translations and rotations.

More formally it is described by a set of commutation relations. Let T_i and R_{ij} be generators of translations and rotations, and let $Q^{(n)}_{i_1 i_2 \cdots i_n}$ be the charge corresponding to the nth multipole moment. The multipole algebra $\mathfrak{M}_{n,k}$ then takes the following form:

$$[T_i, T_j] = 0, \qquad [R_{ij}, T_k] = \delta_{k[i} T_{j]}, \tag{76}$$

$$[R_{ij}, R_{kl}] = \delta_{[k[i} R_{j]l]}, \qquad \left[Q^{(n)}_{i_1 i_2 \cdots i_n}, Q^{(m)}_{i_1 i_2 \cdots i_m}\right] = 0, \tag{77}$$

$$\left[T_j, Q^{(n)}_{i_1 i_2 \cdots i_n}\right] = \sum_{r=1}^{n} \delta_{j i_r} Q^{(n-1)}_{i_1 i_2 \cdots \hat{i}_r \cdots i_n} \quad \forall \ n > k, \tag{78}$$

$$\left[T_j, Q^{(k)}_{i_1 i_2 \cdots i_k}\right] = 0, \tag{79}$$

$$\left[R_{jk}, Q^{(n)}_{i_1 i_2 \cdots i_n}\right] = \sum_{r=1}^{n} \delta_{i_r [j} Q^{(n)}_{k] i_1 \cdots \hat{i}_r \cdots i_n}, \tag{80}$$

where $\hat{i}_r$ indicates that the index i_r should be omitted and $n \geq k$ and the square brackets in Eq. (76) indicate antisymmetrization $\delta_{k[i} T_{j]} = \delta_{ki} T_j - \delta_{kj} T_i$. Equation (79) indicates that $Q^{(k)}_{i_1 i_2 \cdots i_k}$ is the fundamental charge that happens to be a rank-k tensor.

Given the conserved charges $Q^{(n)}_{i_1 i_2 \cdots i_n}$, we postulate a local conservation law in the form of the continuity equation

$$\partial_0 \rho_{i_1 \cdots i_k} + \partial_{i_{n-k}} \cdots \partial_{i_n} J^{i_1 \cdots i_{n-k} \cdots i_n} = 0, \tag{81}$$

where $J^{i_1 \cdots i_{n-k} \cdots i_n}$ is a symmetric tensor current. Equation (81) implies that a tensor charge $Q^{(k)}_{i_1 \cdots i_k}$ is conserved, as are its first $n-k$ moments. In other words, the indivisible unit charge in $\mathfrak{M}_{n,k}$ is a rank-k tensor,

$$Q^{(k)}_{i_1 \cdots i_k} = \int dx \, \rho_{i_1 \cdots i_k}, \tag{82}$$

$$Q^{(m)}_{i_1 \cdots i_m} = \int dx \, x_{i_{k+1}} \cdot \cdots \cdot x_{i_m} \rho_{i_1 \cdots i_k}, \qquad m \leq n-k. \tag{83}$$

We now introduce a set of gauge fields that are conjugate (sourced by) to the tensor charge density $\rho_{i_1 \cdots i_k}$ and the tensor current $J^{i_1 \cdots i_n}$,

$$A_{0, i_1 \cdots i_k}, \qquad A_{i_1 \cdots i_n}. \tag{84}$$

Given these fields, we can modify the Lagrangian of a theory that is invariant under the multipole algebra $\mathfrak{M}_{n,k}$ as follows (this is known as gauging):

$$\delta \mathcal{L} = A_{0, i_1 \cdots i_k} \rho^{i_1 \cdots i_k} + A_{i_1 \cdots i_n} J^{i_1 \cdots i_n}. \tag{85}$$

Therefore, requiring invariance under gauge transformations

$$\delta A_{i_1 \ldots i_n} = \sum_{r=1}^{n} \partial_{i_r} \lambda_{i_1 \ldots \hat{i}_r \ldots i_n}, \tag{86}$$

$$\delta A_{0, i_1 \ldots i_k} = \sum_{r=1}^{n} \partial_0 \lambda_{i_1 \ldots \hat{i}_r \ldots i_n} \tag{87}$$

enforces the continuity equation (81).

The precise structure of Eqs. (86) and (87) depends on k. If the lowest conserved moment is the scalar charge $Q^{(0)}$, i.e., $k = 0$, the gauge parameter takes the following general form:

$$\lambda_{i_1 \ldots i_{n-1}} = \partial_{i_1} \ldots \partial_{i_{n-1}} \lambda. \tag{88}$$

If the lowest conserved moment is $Q^{(k)}_{i_1 i_2 \ldots i_k}$, the algebra still makes sense, assuming that the commutator between translations and $Q^{(k)}_{i_1 i_2 \ldots i_k}$ vanishes: $[T_j, Q^{(k)}_{i_1 i_2 \ldots i_k}] = 0$. If that is the case, we say that the theory has a rank-k tensor charge and the higher moments of this charge are conserved. When $k = 1$ this is known as vector-charge theory.

The density and current can then be found using the usual variational prescription

$$\rho_{i_1 \ldots i_k} = \frac{\delta \mathcal{L}}{\delta A_{0, i_1 \ldots i_k}}, \qquad J^{i_1 \ldots i_n} = \frac{\delta \mathcal{L}}{\delta A_{i_1 \ldots i_n}}. \tag{89}$$

The gauge-invariant electric field $E_{i_1 \ldots i_n}$ is easy to construct. It is given by

$$E_{i_1 \ldots i_n} = \partial_0 A_{i_1 \ldots i_n} - \sum_{r=1}^{n} \partial_{i_r} A_{0, i_1 \ldots \hat{i}_r \ldots i_n}. \tag{90}$$

The Gauss law generating Eq. (90) takes the following form:

$$\partial_{i_{k+1}} \ldots \partial_{i_n} E_{i_1 \ldots i_n} = \rho_{i_1 \ldots i_k}. \tag{91}$$

A gauge-invariant magnetic field can be defined in all of the aforementioned cases; however, its explicit form depends on

the theory and thus we do not provide its general expression. Some tensor gauge theories emerge as a results of spontaneous symmetry breaking of inhomogeneous higher-form symmetries (Hirono *et al.*, 2022).

B. Examples of symmetric tensor gauge theories

The first example is the scalar-charge theory (Pretko, 2017b). It requires the conservation of the dipole moment only. The multipole algebra takes the following form:

$$[T_i, T_j] = 0, \qquad [R_{ij}, T_k] = \delta_{ki} T_j - \delta_{kj} T_i, \tag{92}$$

$$[R_{ij}, R_{kl}] = \delta_{[k[i} R_{j]l]}, \qquad \left[Q_i^{(1)}, Q_j^{(1)}\right] = 0, \tag{93}$$

$$\left[T_i, Q_j^{(1)}\right] = \delta_{ij} Q, \qquad [T_i, Q] = 0, \tag{94}$$

$$\left[R_{jk}, Q_i^{(1)}\right] = \delta_{ki} Q_j^{(1)} - \delta_{kj} Q_i^{(1)}. \tag{95}$$

A field theory invariant under Eqs. (92)–(95) can be readily written. The only degree of freedom is a real scalar ϕ with a Lagrangian given by

$$\mathcal{L} = (\partial_0 \phi)^2 - (\partial_i \partial_j \phi)^2 \tag{96}$$

and is a Lifshitz model with ubiquitous applications (Gorantla *et al.*, 2022; Lake, Hermele, and Senthil, 2022; Radzihovsky, 2022; Stahl, Lake, and Nandkishore, 2022). The Lagrangian (96) is invariant under a polynomial shift symmetry

$$\delta\phi = c_0 + c_i x^i, \tag{97}$$

which by virtue of Noether's theorem implies the conservation of the total charge and total dipole moment. Indeed, there are $d+1$ independent symmetry parameters leading to $d+1$ conserved quantities.

TWe introduce tensor gauge fields into gauge equation (97) as follows:

$$\mathcal{L} = \tfrac{1}{2}(\partial_0 \phi - A_0)^2 - \tfrac{1}{2}(\partial_i \partial_j \phi - A_{ij})^2. \tag{98}$$

The density and tensor current [Eq. (89)] are then given by

$$\rho = \frac{\delta \mathcal{L}}{\delta A_0} = \partial_0 \phi, \qquad J^{ij} = \frac{\delta \mathcal{L}}{\delta A_{ij}} = \partial_i \partial_j \phi \tag{99}$$

and satisfy the continuity equation

$$\partial_0 \rho + \partial_i \partial_j J^{ij} = 0, \tag{100}$$

which implies the dipole conservation.

Our second example is the traceless scalar-charge theory. Its symmetry algebra is a subalgebra of $\mathfrak{M}_2$ where the conserved quantities are

$$Q_i^{(1)}, \qquad \Delta = \mathrm{tr}(Q_{ij}^{(2)}). \tag{101}$$

The only additional nontrivial commutation relation [compared to Eqs. (92)–(95)] is

$$[T_i, \Delta] = Q_i. \tag{102}$$

A Lagrangian invariant under the symmetry algebra (92)–(102) takes the following form:

$$\mathcal{L} = (\partial_0 \phi)^2 - \left(\left[\partial_i \partial_j - \frac{1}{d}\delta_{ij}\partial^2\right]\phi\right)^2. \tag{103}$$

The Lagrangian (103) is invariant under a polynomial shift symmetry

$$\delta\phi = c_0 + c_i x^i + \tilde{c} x_k x^k. \tag{104}$$

The last term in Eq. (104) leads to an extra conservation law for the trace of the quadrupole moment. Gauging leads to a traceless scalar-charge theory with a traceless tensor potential, while the tensor current satisfies an extra constraint $\delta_{ij} J^{ij} = 0$.

Finally, we discuss a general scalar-charge theory that is invariant under the multipole algebra $\mathfrak{M}_{n,0}$. The commutation relations are given by Eqs. (76)–(80) with $k = 0$. The Lagrangian takes the following form:

$$\mathcal{L} = \tfrac{1}{2}(\partial_0 \phi)^2 - \tfrac{1}{2}(\partial_{i_1} \cdots \partial_{i_n} \phi)^2, \tag{105}$$

which is invariant under a general polynomial shift symmetry

$$\delta\phi = c_0 + \sum_{m=1}^{n} c_{i_1 \cdots i_m} x^{i_1} \cdot \cdots \cdot x^{i_m}. \tag{106}$$

The local conservation law that follows from Noether's theorem takes the form of Eq. (81), with $k = 0$.

We introduce a general rank-n tensor gauge field into gauge equation (106) as follows:

$$\mathcal{L} = \tfrac{1}{2}(\partial_0 \phi - A_0)^2 - \tfrac{1}{2}(\partial_{i_1} \ldots \partial_{i_n} \phi - A_{i_1 \ldots i_n})^2. \tag{107}$$

The density and tensor current are then given by Eq. (89), with $k = 0$.

C. General multipole algebra

Thus far we have assumed that the previously discussed tensor gauge theories are invariant under continuous rotations. This does not have to be the case, because we expect at least some of those theories to emerge from UV lattice models and to thereby inherit the lattice symmetries. We restrict our discussion here to scalar-charge theories.

To incorporate the lattice symmetries, we observe that every conserved multipole moment is associated with a polynomial $P(x)$. For example, the conserved dipole moment is associated with d monomials of degree 1: $x_1, x_2, \ldots, x_d$. Generally a component of the multipole tensor $Q_\alpha^{(n)}$ is obtained by integrating a polynomial of degree n $[P_\alpha^{(n)}(x)]$ against the charge density

$$Q_\alpha^{(n)} = \int dx P_\alpha^{(n)}(x) \rho(x). \tag{108}$$

The general index α in Eq. (108) may transform in an irreducible representation of a point group. We now turn to a more formal description of the general multipole algebra.

To describe the algebra we introduce the general multipole moment as follows: Let $P_\alpha^{(n)}(x)$ be a homogeneous polynomial of degree n. The multipole moment corresponding to $P_\alpha^{(n)}(x)$ is then defined as Eq. (108).

Commutation relations between these multipole moments and spatial symmetries form the multipole algebra

$$\left[T_{\hat{\mathbf{r}}}, Q_\alpha^{(n)}\right] = f^{(n)}{}_\alpha{}^\beta Q_\beta^{(n-1)}, \tag{109}$$

$$\left[R_{\hat{\mathbf{r}}}, Q_\alpha^{(n)}\right] = g^{(n)}{}_\alpha{}^\beta Q_\beta^{(n)}, \tag{110}$$

where $T_{\hat{\mathbf{r}}}$ is a translation in direction $\hat{\mathbf{r}}$, $R_{\hat{\mathbf{r}}}$ is the rotation about $\hat{\mathbf{r}}$, and $f^{(n)}{}_\alpha{}^\beta$ and $g^{(n)}{}_\alpha{}^\beta$ are the structure constants. In general, the rotations can either include a subgroup of SO(d) or be discrete. For example, in the gauge theory approach to the Haah code there is an SO(2) rotation symmetry, while $\hat{\mathbf{r}} \propto (1,1,1)$ (Gromov, 2019a).

Given the polynomials, we define a set of homogeneous differential operators D_α that annihilate all $P_I^{(n)}$ simultaneously

$$D_\alpha P_I^{(n)} = 0 \quad \forall \; I, n. \tag{111}$$

The local conservation laws then take form

$$\partial_0 \rho + \sum_\alpha D_\alpha^\dagger J^\alpha = 0, \tag{112}$$

where J^α are the multipole currents and $D_\alpha^\dagger$ is obtained from D_α via integration by parts.

The gauging procedure follows the same logic as in Sec. IV.A. We introduce the gauge fields A_α and A_0 conjugate to the multipole current J^α and density ρ. These gauge fields are labeled as an abstract index (which also can transform into an irreducible representation of the rotation group) and are neither 1-forms nor symmetric tensors. A general Lagrangian invariant under the multipole algebra is supplemented by

$$\delta\mathcal{L} = \rho A_0 + J^\alpha A_\alpha. \tag{113}$$

The gauge transformation law takes the form

$$\delta A_\alpha = D_\alpha \lambda, \qquad \delta A_0 = \partial_0 \lambda \tag{114}$$

and confirms Eq. (112).

Using these D_α, we can construct the electric field and Gauss's law as follows: The electric field is invariant under Eq. (114) and is given by

$$E_\alpha = \partial_0 A_\alpha - D_\alpha A_0, \tag{115}$$

which satisfies Gauss's law with a generalized divergence,

$$\sum_\alpha D_\alpha^\dagger E_\alpha = \rho. \tag{116}$$

D. Relation to the symmetric case

The multipole algebra includes the symmetric case as a special case. Here we illustrate how it works using an example of traceless scalar-charge theory. In d spatial dimensions there are $d+1$ polynomials,

$$P_1^{(1)}(x) = x_1, \ldots, P_d^{(1)}(x) = x_d, \qquad P_1^{(2)}(x) = x_i x^i. \tag{117}$$

The differential operators in Eq. (117) are of degree 2. The index α can be represented as a multi-index $\alpha = (i,j)$, with the differential operators given by

$$D_{i,j} = \partial_i \partial_j - \frac{1}{d}\delta_{ij}\partial^2, \tag{118}$$

where it is clear that Eq. (111) holds; i.e., $D_{i,j}$ annihilates all the polynomials $P_1^{(1)}(x), \ldots, P_d^{(1)}(x), P_1^{(2)}(x)$. This algebra includes all translations and continuous rotations.

E. Gaussian free field with multipole symmetries

Next we discuss an explicit example of a free field theory that is invariant under a general multipole algebra. Consider a real scalar field ϕ and a set of homogeneous polynomials $P_I^{(n)}(x)$. We construct a Lagrangian invariant under the following transformation:

$$\phi \to \phi + P_I^{(n)}(x). \tag{119}$$

To the lowest order in derivatives, the most general action takes the form

$$\mathcal{L} = \tfrac{1}{2}(\partial_0\phi)^2 + \tfrac{1}{2}\sum_\alpha (D_\alpha \phi)^2 \tag{120}$$

by virtue of Eq. (111). The symmetry of Eq. (119) leads to the conservation of Eq. (108).

We can also utilize Eq. (120) to obtain the multipole gauge theory structure. Indeed, the symmetry of Eq. (119) can be gauged by replacing the derivatives as follows:

$$\mathcal{L} = \tfrac{1}{2}(\partial_0\phi - A_0) - \tfrac{1}{2}\sum_\alpha (D_\alpha \phi - A_\alpha)^2, \tag{121}$$

where Φ is the scalar potential. The action (121) is invariant under the gauge transformation (114). The conserved charges are explicitly given by

$$Q_I^{(n)} = \int \partial_0 \phi P_I^{(n)}. \tag{122}$$

F. Multipole gauge theory of a smectic

Next we discuss a simple example of multipole gauge theory that arises as a dual theory to elasticity of a quantum smectic phase (Zhai and Radzihovsky, 2019; Radzihovsky, 2020). We show that a $(2+1)$D quantum smectic is dual to a multipole gauge theory. We start with the following Lagrangian density (De Gennes and Prost, 1993), which

describes a smectic phase at long distances:

$$\mathcal{L} = \tfrac{1}{2}\partial_0 u^2 - \tfrac{1}{2}\kappa(\partial_y u)^2 - \tfrac{1}{2}\kappa(\lambda\partial_x^2 u)^2, \tag{123}$$

where the layers are perpendicular to the y axis and extend along the x axis. We reiterate that a smectic is a liquid crystal phase that spontaneously breaks rotational symmetry (by the choice of layer orientation) and one out of the two translation symmetries. It can be viewed as a periodic array of 1D liquids with a period of order λ along the y axis. We denote

$$D_1^\dagger = \partial_x, \qquad D_2^\dagger = \lambda\partial_y^2. \tag{124}$$

In terms of these derivatives the action is

$$\mathcal{L} = \tfrac{1}{2}\partial_0 u^2 - \tfrac{1}{2}\kappa(D_1^\dagger u)^2 - \tfrac{1}{2}\kappa(D_2^\dagger u)^2. \tag{125}$$

We introduce auxiliary variables using the Hubbard-Stratonovich trick as

$$\mathcal{L} = P\dot{u} - \frac{P^2}{2} - (D_1^\dagger u)T_1 - (D_2^\dagger u)T_2 + \epsilon\frac{T_1^2}{2} + \epsilon\frac{T_2^2}{2}. \tag{126}$$

Integrating out the phonon u, we find the constraint

$$\partial_0 P - D_1 T_1 - D_2 T_2 = 0. \tag{127}$$

Equation (127) is solved using

$$T_I = \epsilon_{IJ}(\partial_0 A_J - D_J A_0) = \epsilon_{IJ}E_J, \tag{128}$$

$$P = B = \epsilon_{IJ}D_I A_J, \tag{129}$$

where ϵ_{IJ} is the Levi-Civita symbol and $I, J = 1$ and 2. The gauge redundancy of the solution is

$$\delta A_I = D_I\lambda, \qquad \delta A_0 = \dot{\lambda}, \tag{130}$$

which is exactly a multipole gauge theory structure. The Gauss law that generates Eq. (130) is given by

$$D_I^\dagger E_I = \rho. \tag{131}$$

The defect density ρ is the density of smectic disclinations. The defect matter conserves the dipole moment in the u direction, which can be seen directly in Eq. (131). The disclination dipole extended in the u direction is a dislocation with the Burgers vector in the w direction. The dislocations are completely mobile (Kleman and Lavrentovich, 2003), whereas the disclinations are 1D particles (also known as lineons) that can move only in the w direction. The low-energy phonon is described by the multipole gauge theory with the generalized Maxwell action

$$\mathcal{L} = \tfrac{1}{2}\epsilon(E_1^2 + E_2^2) - \tfrac{1}{2}B^2. \tag{132}$$

As required, $\mathcal{L}$ admits a single smectic mode with a linear dispersion along the y axis and a quadratic dispersion along the x axis.

G. U(1) Haah code in three dimensions

Next we turn to a discussion of the "U(1) Haah code" studied by Bulmash and Barkeshli (2018b) and Gromov (2019a). We begin by postulating the symmetries

$$\delta\phi = c_0 + c_1 P_1^{(1)} + c_2 P_2^{(1)} + c_3 P_1^{(2)} + c_4 P_2^{(2)}, \tag{133}$$

where

$$P_1^{(1)} = x_1 - x_2, \qquad P_2^{(1)} = x_1 + x_2 - 2x_3, \tag{134}$$

$$P_1^{(2)} = (x_1 - x_2)(x_1 + x_2 - 2x_3), \tag{135}$$

$$P_2^{(2)} = (2x_1 - x_2 - x_3)(x_2 - x_3). \tag{136}$$

These polynomials were chosen after the elementary fracton configurations in the Haah code were examined (Gromov, 2019a) and generalized to the U(1) conserved charge. These configurations carry the dipole moment in the $(1, 1, 1)$ direction, which leads us to enforce conservation of the dipole moment in the (111) plane. Polynomials of degree 2 were chosen in a similar manner. We also enforce the SO(2) symmetry in the (111) plane. This leaves us with three invariant derivatives that take the following forms:

$$D_1 = q^i\partial_i, \quad D_2 = q_1^{ij}\partial_i\partial_j, \quad D_3 = q_2^{ij}\partial_i\partial_j, \tag{137}$$

where

$$q^i = \begin{pmatrix}1\\1\\1\end{pmatrix}, \quad q_1^{ij} = \begin{pmatrix}1&0&0\\0&1&0\\0&0&1\end{pmatrix}, \quad q_2^{ij} = \begin{pmatrix}0&1/2&1/2\\1/2&0&1/2\\1/2&1/2&0\end{pmatrix}.$$

The elementary charge configurations are shown in Fig. 13.

We then gauge these symmetries as previously explained. The Lagrangian describing dynamics of the gauge field is given by

$$\mathcal{L} = \sum_I E_I^2 - B_1^2 - B_2^2, \tag{138}$$

where the magnetic fields are given by

$$B_I = \epsilon_{IJK}D_J A_K \tag{139}$$

and the Gauss law takes the following form:

$$\sum_\beta D_\beta^\dagger E_\beta = \rho. \tag{140}$$

The U(1) Haah model has a hidden infinite symmetry. We now introduce a bit of notation. To begin, we define a basis μ_i^1, μ_i^2 in the plane where the dipole moment is conserved. One choice is $\mu^1 = (1, -1, 0)$ and $\mu^2 = (1, 1, -2)$. With this basis at hand we introduce new variables $x = \mu_i^1 x^i/|\mu^1|$ and

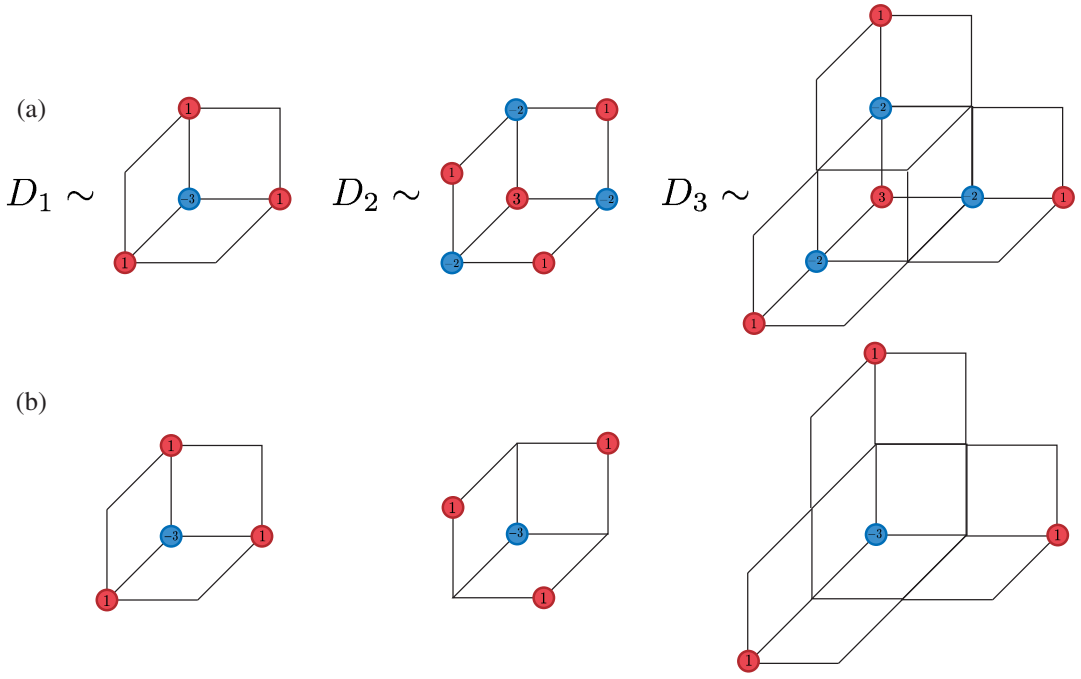

FIG. 13. (a) Elementary charge configurations corresponding to the invariant derivatives D_I for the effective theory for the U(1) Haah code (137) charge configurations. These charge configurations violate conservation of the dipole moment in the $(1, 1, 1)$ direction. (b) A different basis of elementary charge configurations. The first two configurations are those studied by Bulmash and Barkeshli (2018b), while the last charge configuration is allowed by symmetries and is linearly independent of the others.

$y = \mu_i^2 x^i/|\mu^2|$. All invariant derivatives D_α (and consequently the Lagrangian) are also invariant under an infinite symmetry

$$\delta\phi(z, \bar{z}, x_3) = f(z) + g(\bar{z}), \qquad z = x + iy, \tag{141}$$

where $f(z)$ is holomorphic and $g(\bar{z})$ is antiholomorphic. This is an example of the well-known "sliding" symmetry (Barci *et al.*, 2002) that appears in the physics of smectics (O'Hern and Lubensky, 1998); it can be understood as a continuous version of subsystem symmetries. Finally, the U(1) Haah model exhibits an anisotropic scaling symmetry that takes the following form:

$$t \to \lambda t, \quad x \to \lambda^{1/2} x, \quad y \to \lambda^{1/2} y, \quad x_3 \to \lambda x_3, \quad \phi \to \lambda^{-1/2}\phi. \tag{142}$$

Gromov (2020) showed that the gauge theory for the U(1) Haah code (138) is dual to the smectic-*A* phase in three dimensions.

H. Subsystem symmetry

We now turn to an even more exotic class of much larger, more extensive symmetries: the so-called subsystem symmetries, which lead to restricted mobility and multipole gauge theories upon gauging (Vijay, Haah, and Fu, 2015, 2016). These symmetries were initially defined on a lattice for various spin models, but as we illustrate they can be extended to the continuum.

While a covariant theory of subsystem symmetries has not yet been developed, we can understand a class of these symmetries as an infinite-dimensional generalization of the multipole algebra discussed in Sec. IV.G. In our development we assume that the physical model is defined on a flat space and that we are given a set of lines, planes, or hyperplanes that foliate the space.

As a pedagogical example, we consider a model of a real scalar field in two dimensions $\phi(x_1, x_2)$, with the following transformation being an example of subsystem symmetry:

$$\delta\phi = f_1(x_1) + f_2(x_2), \tag{143}$$

where $f_1(x_1)$ and $f_2(x_2)$ are arbitrary functions of x_1 and x_2. The set of lines consists of two families: (i) lines parallel to x_2 and (ii) lines parallel to x_1. Any 2D lattice provides enough structure to develop a set of subsystem symmetries.

The algebra of subsystem symmetries is infinite dimensional. Its action is intermediate between a global symmetry that acts on full d-dimensional space and gauge redundancy that acts on individual sites. We can also interpret it as an infinite-dimensional generalization of the multipole algebra by representing the functions f_1 and f_2 as the Taylor series in x_1 and x_2, respectively,

$$\delta\phi = \sum_{n\geq 0} c_n x_1^n + \sum_{m\geq 0} b_m x_2^m, \tag{144}$$

where c_n and b_m are arbitrary coefficients. Viewed this way, the symmetry implies conservation of arbitrary high multipole moments in one of the axes,

$$Q^{(n)}_{11\ldots1}, \quad Q^{(n)}_{22\ldots2}, \quad n \geq 0. \tag{145}$$

The Lagrangian invariant under Eq. (143) breaks rotational symmetry down to a discrete subgroup C_4,

$$\mathcal{L} = \tfrac{1}{2}(\partial_0\phi)2 - \tfrac{1}{2}(\partial_1\partial_2\phi)^2 + \cdots \tag{146}$$

and was analyzed by Gorantla *et al.* (2022).

Subsystem symmetries can also be gauged. Indeed, gauging Eq. (143) requires a single "vector" potential A_{12} that transforms as $\delta A_{12} = \partial_1\partial_2\lambda$. There is a single electric field given by $E_{12} = \partial_0 A_{12} - \partial_1\partial_2 A_0$ and the Gauss law takes the following form:

$$\partial_1\partial_2 E_{12} = \rho. \tag{147}$$

Other examples of subsystem symmetries were discussed by Gromov, Lucas, and Nandkishore (2020).

The conservation law following from Eq. (143) is encoded in the continuity equation

$$\partial_0\rho + \partial_1\partial_2 J = 0, \tag{148}$$

where J is the current. It exhibits an infinite number of conserved charges

$$Q_{1x} = \int_{x_1=x} dx_2\rho(x_1,x_2), \quad Q_{2y} = \int_{x_2=y} dx_1\rho(x_1,x_2) \tag{149}$$

that are conserved independently on any lines x and y, respectively. It is thus clear that this conservation law makes particles that are charged under both Q_{1x} and Q_{2y} completely immobile, while the dipoles can move perpendicularly to their dipole moments.

I. Fracton hydrodynamics

Conservation laws (25) and (148) can in principle be either microscopic or emergent. In either case, the long-wave, long-time phenomenology is affected if these conservation laws are present. These effects manifest themselves in the transport of charge and momentum, with the simplest manifestation being subdiffusion.

We illustrate the emergence of subdiffusion in the simplest case of a conserved dipole moment. As discussed, the corresponding charge continuity equation takes the following form [Eq. (25)]:

$$\partial_0\rho + \partial_i\partial_j J^{ij} = 0. \tag{150}$$

To describe diffusion of charge, we relate the dipole current to the charge density. In equilibrium the dipole current must vanish. Consequently, the constitutive relation between ρ and J^{ij} takes the form

$$J^{ij} = \chi^{-1}\partial^i\partial^j\rho + \cdots, \tag{151}$$

where χ is the susceptibility. The (sub)diffusion equation then takes the form

$$\partial_0\rho + \chi\partial^4\rho = 0. \tag{152}$$

Equation (152) implies that the density perturbation at wavelength λ will decay at a characteristic time $\tau \sim \chi\lambda^4$ (Pretko and Radzihovsky, 2018a; Gromov, Lucas, and Nandkishore, 2020; Radzihovsky and Hermele, 2020; Radzihovsky, 2020) for long wavelengths that are parametrically far slower than the conventional diffusive time $\sim\lambda^2$. Such slow relaxation time enhancement has been observed in cold atomic gasses in tilted optical lattices (Guardado-Sanchez *et al.*, 2020). Subdiffusion also emerges in random unitary circuits (Iaconis, Vijay, and Nandkishore, 2019; Feldmeier *et al.*, 2020; Moudgalya *et al.*, 2021).

Such subdiffusion straightforwardly generalizes to the case of conservation of the nth multipole moment, where it gives

$$\partial_0\rho + \chi\partial^{2+2n}\rho = 0, \tag{153}$$

leading to an even slower characteristic time $\tau \sim \chi\lambda^{2+2n}$.

Another interesting effect occurs when the subsystem symmetry constrains the diffusion equation. Consider the charge conservation equation (148) with dipole symmetry. Relating the generalized current to the density with the subsystem constraint, we obtain the (sub)diffusion equation

$$\partial_0\rho + \chi^{-1}\partial_x^2\partial_y^2\rho = 0. \tag{154}$$

Thus, the subsystem symmetry breaks the rotational symmetry down to a discrete subgroup of the lattice, with these effects persisting at the longest scales. This is in stark contrast to classic diffusion, which has an emergent rotational symmetry to the lowest order in derivatives.

V. CONCLUSIONS

A. Summary

In this Colloquium we reviewed the theoretically inspired, burgeoning subject of fractonic matter. We began with a model-independent, symmetry- and conservation-based formulation of fractons: excitations with restricted mobility arising in a broad class of exotic models.

The central focus of this Colloquium is the emergence of fractonic order from elasticity-gauge duality of a broad class of quantum elasticity models that include quantum commensurate and incommensurate supersolid crystals, smectic liquid crystals, hexatic fluids, amorphous solids, quasicrystals, and elastic membranes, all of which encode some form of multipolar global symmetry. We also discussed a vortex crystal and a vortex liquid that dualize to parity-breaking gauge-dual variants. Building on the familiar boson-vortex duality, we explicitly reviewed how such dualities lead to interesting tensor and coupled-vector gauge theories that exhibit fractonic charges, dipoles, and higher multipoles as duals of elastic topological defects, with gauge fields encoding gapless phonons.

As discussed, such elasticity-gauge duality is a powerful tool for discovery of a new class of fractonic models. The resulting models can then be generalized into a broader class beyond any elastic dual connection. A complementary motivation for the duality studies is that they provide an efficient formulation of the quantum elasticity and the topological

defect dynamics. One striking example is the prediction of the zero-temperature immobility of disclinations in a 2D crystal (previously unknown despite decades of studies of it in the elasticity context) that arose purely through this fractonic gauge theory connection. In the Colloquium, we furthermore demonstrated that gauge duals provide a field-theoretic formulation of quantum melting of a crystal and a smectic through a generalized Higgs mechanism associated with a condensation of dislocations and disclinations.

As discussed, tensor gauge theories can be studied in arbitrary dimensions and without any relation to elasticity. We presented a general construction of a large class of such gauge theories based on gauging the multipole algebra, an algebra of spatial symmetries that includes dipole and higher multipole symmetries. The resulting multipole gauge theories include models obtained from dualities as special cases. We expect these theories to serve as templates for identifying exotic gapless excitations in spin liquids.

We also discussed even more exotic subsystem symmetries and illustrated a formal relation between these symmetries and infinite-dimensional multipole algebras. We concluded the Colloquium with a description of the long-time subdiffusive hydrodynamics of fractonic matter that emerges as a result of multipole conservation laws.

B. Open problems

While the field of fractons and associated tensor and multipole gauge theories has seen rapid growth in the past ten years, it remains in an early stage of development, with many open theoretical and experimental questions.

1. Mathematical structure

Most fundamentally the mathematical structure of tensor gauge theories is still not well formulated. It is currently unclear as to what will replace the G bundle of traditional gauge theories. Consequently, the topology of the space of tensor gauge fields is poorly understood. Namely, since the geometric interpretation of tensor gauge fields is unclear, it is not known how to construct topological invariants that generalize Chern numbers. In fact, it is certain that such invariants cannot be purely topological, because any naive generalization of the Chern number will depend on the spatial metric, leading to the metric dependence of the "topological invariant." One can also generalize the Chern-Simons theory to the higher-rank case, but the dependence on the metric appears to be unavoidable. Furthermore, in all cases the inclusion of the metric is in tension with gauge invariance, with the magnetic field found to be gauge invariant only in flat space (or on an Einstein manifold in certain cases) (Gromov, 2019b; Slagle, Prem, and Pretko, 2019; Bidussi *et al.*, 2022; Jain and Jensen, 2022). One hopes, however, that a coupled-vector gauge theory formulation (Radzihovsky and Hermele, 2020; Radzihovsky, 2020) will be more suitable for addressing these questions.

As discussed in the Introduction, fractonic gauge theories concisely encode quasiparticle restricted mobility and Gaussian fluctuations. However, these continuum field theories preclude an encoding of their expected exponential in-system-size ground-state degeneracy[15] and nontrivial quasiparticle quantum statistics (Qi, Radzihovsky, and Hermele, 2021). This contrasts strongly with discrete qubit models (such as X-cube), where these properties are well defined and have been calculated (Bulmash and Barkeshli, 2018a; Ma, Hermele, and Chen, 2018).

As recently demonstrated (Doshi and Gromov, 2021; Du *et al.*, 2022), a gauge structure and phenomenology similar to that of fractonic tensor gauge theories also arises in superfluids and with the fractional quantum Hall effect. In fact, a similar form and UV-IR mixing characteristic of fractonic gauge theories (Gorantla *et al.*, 2022) arise in the noncommutative gauge theories as well as noncommutative matter theories coupled to a gauge field. The development and illumination of these relations remain open problems.

2. Quantum melting and insights on elasticity

Focusing on specific models and their phenomenology as discussed in this Colloquium, we saw that these dual gauge theories are also of interest because they provide a formulation of crystal-to-hexatic, crystal-to-smectic, smectic-to-nematic quantum melting transitions as a generalized Higgs transition associated with a condensation of the topological defects. However, these have thus far been analyzed only at the mean-field level, thus leaving their true criticality to future studies.

3. Generalizations beyond bosonic elasticity

We note that, in all of the elastic models reviewed here and studied in the literature, the focus has been on the simplest bosonic realizations. These have led to bosonic statistics of dislocation and disclination defects (i.e., bosonic fracton matter) and superfluidity when crystalline order is lost. It is natural to study extensions of the bosonic duality to that of fermions and anyons and to explore the possibility of nontrivial statistics of topological defects.

4. Experimental void

The field's most vexing challenge is that of experimental realizations, which thus far have been absent. In part this is due to the fact that discrete qubit (for example, the simplest X-cube) models are typically formulated in terms of many-spin commuting projectors, which are therefore extremely difficult to implement. A promising alternative direction is that of the $\mathrm{U}(1)$ tensor and coupled-vector gauge theories that have been the focus of this Colloquium. These are related to discrete models through the condensation of higher charge matter (Bulmash and Barkeshli, 2018a; Ma, Hermele, and Chen, 2018). In fact, the $(2+1)$D crystal-gauge duality demonstrates a concrete physical realization of fractonic order in a familiar quantum crystal and in other elastic media.

In tensor gauge theories, realization-independent quadrupolar pinch-point singularities have been predicted (Prem *et al.*, 2018; Nampoothiri *et al.*, 2020; Nandkishore, Choi, and Kim, 2021; Hart and Nandkishore, 2022), extending neutron

[15]That is, unless lattice regularization is introduced (Slagle and Kim, 2017b; Rudelius, Seiberg, and Shao, 2021; Seiberg and Shao, 2021).

scattering predictions for conventional spin liquids in frustrated magnets (Savary and Balents, 2017), and in fact have been observed in granular solids (Behringer and Chakraborty, 2019). However, to date no smoking gun restricted mobility experiments have been conceived, even in these physical instantiations of an in-principle fractonic elastic system. The immobility of disclinations is not a particularly impressive observation, especially deep inside a crystal phase, where even vacancies and interstitials are energetically immobile and behave classically. Perhaps a study of a ^{4}He crystalline film or 2D lattices of ultracold bosons close to a low-temperature quantum melting transition would be a good experimental platform to explore.

Another obstacle in this area is that in two dimensions the disclination energy is extensively large and thus is not an excitation that is easy to explore. In contrast, the topology of a spherical crystal, such as the buckminsterfullerene C_{60} molecule, and many other closed structures (as large as C_{960}), using the Gauss-Bonnet theorem automatically ensures 12 disclinations in the ground state, whose lattice hopping dynamics could perhaps be studied experimentally. The extension of dual gauge theories to a spherical geometry with a detailed analysis remains an open problem, and corresponding experiments would be an interesting direction to pursue.

Some further proposals for experimental realization of fractons or tensor gauge fields have been made for spin liquids (Yan *et al.*, 2020), Rydberg atoms (Verresen, Tantivasadakarn, and Vishwanath, 2021; Myerson-Jain *et al.*, 2022), and Ising antiferromagnets (Sous and Pretko, 2020a, 2020b). This plethora of interesting open problems bodes well for a bright future in the engaging field of fractons, a current glimpse of which we presented in this Colloquium.

ACKNOWLEDGMENTS

L. R. thanks Mike Hermele, Michael Pretko, Marvin Qi, and Zhengzheng Zhai for the collaborations. L. R. acknowledges the support of the Simons Investigator Award from the Simons Foundation. A. G. is supported by NSF CAREER Grant No. DMR-2045181, the Sloan Foundation, and the Laboratory for Physical Sciences through the Condensed Matter Theory Center.

REFERENCES

Aasen, D., D. Bulmash, A. Prem, K. Slagle, and D. J. Williamson, 2020, "Topological defect networks for fractons of all types," Phys. Rev. Res. **2**, 043165.

Albert, V. V., S. Pascazio, and M. H. Devoret, 2017, "General phase spaces: From discrete variables to rotor and continuum limits, J. Phys. A **50**, 504002.

Ardonne, E., P. Fendley, and E. Fradkin, 2004, "Topological order and conformal quantum critical points, Ann. Phys. (N.Y.) **310**, 493–551.

Barci, D. G., E. Fradkin, S. A. Kivelson, and V. Oganesyan, 2002, "Theory of the quantum Hall smectic phase. I. Low-energy properties of the quantum Hall smectic fixed point," Phys. Rev. B **65**, 245319.

Beekman, Aron J., Jaakko Nissinen, Kai Wu, Ke Liu, Robert-Jan Slager, Zohar Nussinov, Vladimir Cvetkovic, and Jan Zaanen, 2017, "Dual gauge field theory of quantum liquid crystals in two dimensions," Phys. Rep. **683**, 1–110.

Behringer, R. P., and B. Chakraborty, 2019, "The physics of jamming for granular materials: A review," Rep. Prog. Phys. **82**, 012601.

Bi, D., J. Zhang, B. Chakraborty, and R. P. Behringer, 2011, "Jamming by shear," Nature (London) **480**, 355–358.

Bidussi, L., J. Hartong, E. Have, J. Musaeus, and S. Prohazka, 2022, "Fractons, dipole symmetries and curved spacetime," SciPost Phys., **12**, 205.

Blagojevic, M., and F. W. Hehl, 2012, "Gauge theories of gravitation," arXiv:1210.3775.

Bravyi, S., and J. Haah, 2013, "Quantum Self-Correction in the 3D Cubic Code Model," Phys. Rev. Lett. **111**, 200501.

Bravyi, S., B. Leemhuis, and B. M. Terhal, 2011, "Topological order in an exactly solvable 3D spin model," Ann. Phys. (N.Y.) **326**, 839–866.

Bulmash, D., and M. Barkeshli, 2018a, "Higgs mechanism in higher-rank symmetric U(1) gauge theories," Phys. Rev. B **97**, 235112.

Bulmash, D., and M. Barkeshli, 2018b, "Generalized U(1) gauge field theories and fractal dynamics," arXiv:1806.01855.

Caddeo, A., C. Hoyos, and D. Musso, 2022, "Emergent dipole gauge fields and fractons," arXiv:2206.12877.

Castelnovo, C., and C. Chamon, 2012, "Topological quantum glassiness," Philos. Mag. **92**, 304–323.

Chaikin, P. M., and T. C. Lubensky, 1995, *Principles of Condensed Matter Physics* (Cambridge University Press, Cambridge, England).

Chamon, C., 2005, "Quantum Glassiness in Strongly Correlated Clean Systems: An Example of Topological Overprotection," Phys. Rev. Lett. **94**, 040402.

Dasgupta, C., and B. I. Halperin, 1981, "Phase Transition in a Lattice Model of Superconductivity," Phys. Rev. Lett. **47**, 1556.

De Gennes, P. G., and J. Prost, 1993, *The Physics of Liquid Crystals*, International Series of Monographs on Physics Vol. 83 (Oxford University Press, New York).

Devakul, Trithep, S. A. Parameswaran, and S. L. Sondhi, 2018, "Correlation function diagnostics for type-I fracton phases," Phys. Rev. B **97**, 041110.

Ding, D., W. Yang, C. Hu, and R. Wang, 1993," Generalized elasticity theory of quasicrystals," Phys. Rev. B **48**, 7003.

Doshi, D., and A. Gromov, 2021, "Vortices as fractons," Commun. Phys. **4**, 44.

Du, Y. H., U. Mehta, D. Nguyen, and D. T. Son, 2022, "Volume-preserving diffeomorphism as nonabelian higher-rank gauge symmetry" SciPost Phys. **12**, 050.

Else, D. V., S. J. Huang, A. Prem, and A. Gromov, 2021, "Quantum Many-Body Topology of Quasicrystals," Phys. Rev. X **11**, 041051.

Feldmeier, J., P. Sala, G. De Tomasi, F. Pollmann, and M. Knap, 2020, "Anomalous Diffusion in Dipole- and Higher-Moment-Conserving Systems," Phys. Rev. Lett. **125**, 245303.

Fisher, M. P. A., and D. H. Lee, 1989, "Correspondence between two-dimensional bosons and a bulk superconductor in a magnetic field," Phys. Rev. B **39**, 2756.

Fradkin, E., D. A. Huse, R. Moessner, V. Oganesyan, and S. L. Sondhi, 2004, "Bipartite Rokhsar-Kivelson points and Cantor deconfinement," Phys. Rev. B **69**, 224415.

Fradkin, E., and S. Kivelson, 1999, "Liquid-crystal phases of quantum Hall systems," Phys. Rev. B **59**, 8065.

Fulde, P., and R. A. Ferrell, 1964, "Superconductivity in a strong spin-exchange field," Phys. Rev. **135**, A550.

Gaa, J., G. Palle, R. M. Fernandes, and J. Schmalian, 2021, "Fracton-elasticity duality in twisted moiré superlattices," Phys. Rev. B **104**, 064109.

Geng, J., D. Howell, E. Longhi, R. P. Behringer, G. Reydellet, L. Vanel, E. Clément, and S. Luding, 2001, "Footprints in Sand: The Response of a Granular Material to Local Perturbations," Phys. Rev. Lett. **87**, 035506.

Glorioso, P., J. Guo, J. F. Rodriguez-Nieva, and A. Lucas, 2022, "Breakdown of hydrodynamics below four dimensions in a fracton fluid," Nat. Phys., **18**, 912–917.

Gorantla, Pranay, Ho Tat Lam, Nathan Seiberg, and Shu-Heng Shao, 2022, "2 + 1D compact Lifshitz theory, tensor gauge theory, and fractons," arXiv:2201.10589.

Gromov, A., 2019a, "Towards Classification of Fracton Phases: The Multipole Algebra," Phys. Rev. X **9**, 031035.

Gromov, A., 2019b, "Chiral Topological Elasticity and Fracton Order," Phys. Rev. Lett. **122**, 076403.

Gromov, A., 2020, "A duality between U(1) Haah code, and 3D smectic-*A* phase," arXiv:2002.11817.

Gromov, A., A. Lucas, and R. Nandkishore, 2020, "Fracton hydrodynamics," Phys. Rev. Res. **2**, 033124.

Gromov, A., and P. Surowka, 2020, "On duality between Cosserat elasticity and fractons," SciPost Phys. **8**, 065.

Grosvenor, K. T., C. Hoyos, F. Peña-Benítez, and P. Surówka, 2022, "Space-dependent symmetries and fractons," Front. Phys. **9**, 792621.

Guardado-Sanchez, E., A. Morningstar, B. M. Spar, P. T. Brown, D. A. Huse, and W. S. Bakr, 2020, "Subdiffusion and Heat Transport in a Tilted Two-Dimensional Fermi-Hubbard System," Phys. Rev. X **10**, 011042.

Guo, J., P. Glorioso, and A. Lucas, 2022, "Fracton Hydrodynamics without Time-Reversal Symmetry," Phys. Rev. Lett. **129**, 150603.

Haah, J., 2011, "Local stabilizer codes in three dimensions without string logical operators," Phys. Rev. A **83**, 042330.

Haah, J., 2013a, *Lattice Quantum Codes and Exotic Topological Phases of Matter* (California Institute of Technology, Pasadena).

Haah, J., 2013b, "Commuting Pauli Hamiltonians as maps between free modules," Commun. Math. Phys. **324**, 351–399.

Haah, J., 2014, "Bifurcation in entanglement renormalization group flow of a gapped spin model," Phys. Rev. B **89**, 075119.

Haah, J., 2016, "Algebraic methods for quantum codes on lattices," Rev. Colomb. Mat. **50**, 299–349.

Haah, J., 2021, "A degeneracy bound for homogeneous topological order," SciPost Phys. **10**, 011.

Halász, G. B., T. H. Hsieh, and L. Balents, 2017, "Fracton Topological Phases from Strongly Coupled Spin Chains," Phys. Rev. Lett. **119**, 257202.

Halperin, B. I., T. C. Lubensky, and S. K. Ma, 1974, "First-Order Phase Transitions in Superconductors and Smectic-*A* Liquid Crystals," Phys. Rev. Lett. **32**, 292.

Halperin, B. I., and D. R. Nelson, 1978, "Theory of Two-Dimensional Melting," Phys. Rev. Lett. **41**, 121.

Hart, O., and R. M. Nandkishore, 2022, "Spectroscopic fingerprints of gapless type-II fracton phases," Phys. Rev. B **105**, L180416.

He, H., Y. Zheng, B. A. Bernevig, and N. Regnault, 2018, "Entanglement entropy from tensor network states for stabilizer codes," Phys. Rev. B **97**, 125102.

Hirono, Y., M. You, S. Angus, and G. Y. Cho, 2022, "A symmetry principle for gauge theories with fractons," arXiv:2207.00854.

Hsieh, T. H., and G. B. Halász, 2017, "Fractons from partons," Phys. Rev. B **96**, 165105.

Hsieh, Tzu-Chi, Han Ma, and Leo Radzihovsky, 2022, "Helical superfluid in a frustrated honeycomb Bose-Hubbard model," Phys. Rev. A **106**, 023321.

Iaconis, J., S. Vijay, and R. M. Nandkishore, 2019, "Anomalous subdiffusion from subsystem symmetries," Phys. Rev. B **100**, 214301.

Jain, A., and K. Jensen, 2022, "Fractons in curved space," SciPost Phys., **12**, 142.

Kalugin, P. A., A. I. Kitaev, and L. S. Levitov, 1985, "$Al_{0.86}Mn_{0.14}$: A six-dimensional crystal," ZhETF Pis'ma v Redaktsiyu, **41**, 145–149.

Kapustin, A., and L. Spodyneiko, 2022, "Hohenberg-Mermin-Wagner-type theorems and dipole symmetry," arXiv:2208.09056.

Katanaev, M. O., and I. V. Volovich, 1992, "Theory of defects in solids and three-dimensional gravity," Ann. Phys. (N.Y.), **216**, 1–28.

Kivelson, S. A., E. Fradkin, and V. J. Emery, 1998, "Electronic liquid crystal phases of a doped Mott insulator," Nature (London) **393**, 550–553.

Kleinert, H., 1983, "Dual model for dislocation and disclination melting," Phys. Lett. **96A**, 302–306.

Kleinert, H., 1989, *Gauge Fields in Condensed Matter, Vol. I: Stress and Defects* (World Scientific, Singapore).

Kleinert, H., 2008, *Multivalued Fields in Condensed Matter, Electromagnetism, and Gravitation* (World Scientific, Singapore).

Kleman, M., and O. D. Lavrentovich, 2003, *Soft Matter Physics: An Introduction* (Springer, New York).

Kondo, K., 1949, "A proposal of a new theory concerning the yielding of materials based on Riemannian geometry, I," J. Soc. Appl. Mech. Jpn. **2**, 123–128, https://www.jstage.jst.go.jp/article/jjsass1948/2/11/2_11_123/_pdf.

Kosterlitz, J. M., and D. J. Thouless, 1973, "Ordering, metastability and phase transitions in two-dimensional systems," J. Phys. C **6**, 1181.

Koulakov, A. A., M. M. Fogler, and B. I. Shklovskii, 1996, "Charge Density Wave in Two-Dimensional Electron Liquid in Weak Magnetic Field," Phys. Rev. Lett. **76**, 499.

Kozii, Vladyslav, Jonathan Ruhman, Liang Fu, and Leo Radzihovsky, 2017, "Ferromagnetic transition in a one-dimensional spin-orbit-coupled metal and its mapping to a critical point in smectic liquid crystals," Phys. Rev. B **96**, 094419.

Kumar, Ajesh, and Andrew C. Potter, 2019, "Symmetry-enforced fractonicity and two-dimensional quantum crystal melting," Phys. Rev. B **100**, 045119.

Lake, E., M. Hermele, and T. Senthil, 2022, "Dipolar Bose-Hubbard model," Phys. Rev. B **106**, 064511.

Lake, Ethan, Hyun-Yong Lee, Jung Hoon Han, and T. Senthil, 2022, "Dipole condensates in tilted Bose-Hubbard chains," arXiv:2210.02470.

Landau, L. D., E. M. Lifshitz, and A. M. Kosevich, 1986, *Theory of Elasticity*, Course of Theoretical Physics Vol. 7 (Elsevier, New York).

Larkin, A. I., and Yu. N. Ovchinnikov, 1965, "Nonuniform state of superconductors," Sov. Phys. JETP **20**, 762.

Le Doussal, Pierre, and Leo Radzihovsky, 2018, "Anomalous elasticity, fluctuations and disorder in elastic membranes," Ann. Phys. (N.Y.) **392**, 340–410.

Levine, D., and P. J. Steinhardt, 1984, "Quasicrystals: A New Class of Ordered Structures," Phys. Rev. Lett. **53**, 2477.

Lilly, M. P., K. B. Cooper, J. P. Eisenstein, L. N. Pfeiffer, and K. W. West, 1999, "Evidence for an Anisotropic State of Two-Dimensional Electrons in High Landau Levels," Phys. Rev. Lett. **82**, 394.

Lubensky, T. C., S. Ramaswamy, and J. Toner, 1985, "Hydrodynamics of icosahedral quasicrystals," Phys. Rev. B **32**, 7444.
Ma, H., M. Hermele, and X. Chen, 2018, "Fracton topological order from the Higgs and partial-confinement mechanisms of rank-two gauge theory," Phys. Rev. B **98**, 035111.
Ma, H., E. Lake, X. Chen, and M. Hermele, 2017, "Fracton topological order via coupled layers," Phys. Rev. B **95**, 245126.
Ma, H., and M. Pretko, 2018, "Higher rank deconfined quantum criticality at the Lifshitz transition and the exciton Bose condensate," Phys. Rev. B **98**, 125105.
Ma, H., A. T. Schmitz, S. A. Parameswaran, M. Hermele, and R. M. Nandkishore, 2018, "Topological entanglement entropy of fracton stabilizer codes," Phys. Rev. B **97**, 125101.
MacDonald, A. H., and Matthew P. A. Fisher, 2000, "Quantum theory of quantum Hall smectics," Phys. Rev. B **61**, 5724.
Manoj, N., R. Moessner, and V. B. Shenoy, 2021, "Fractonic View of Folding and Tearing Paper: Elasticity of Plates Is Dual to a Gauge Theory with Vector Charges," Phys. Rev. Lett. **127**, 067601.
Marchetti, M. C., and L. Radzihovsky, 1999, "Interstitials, vacancies, and dislocations in flux-line lattices: A theory of vortex crystals, supersolids, and liquids," Phys. Rev. B **59**, 12001.
Moessner, R., and J. T. Chalker, 1996, "Exact results for interacting electrons in high Landau levels," Phys. Rev. B **54**, 5006.
Moudgalya, S., A. Prem, D. A. Huse, and A. Chan, 2021, "Spectral statistics in constrained many-body quantum chaotic systems," Phys. Rev. Res. **3**, 023176.
Myerson-Jain, N. E., S. Yan, D. Weld, and C. Xu, 2022, "Construction of Fractal Order and Phase Transition with Rydberg Atoms," Phys. Rev. Lett. **128**, 017601.
Nakahara, M., 2018, *Geometry, Topology and Physics* (CRC Press, Boca Raton).
Nampoothiri, J. N., Y. Wang, K. Ramola, J. Zhang, S. Bhattacharjee, and B. Chakraborty, 2020, "Emergent Elasticity in Amorphous Solids," Phys. Rev. Lett. **125**, 118002.
Nandkishore, R. M., W. Choi, and Y. B. Kim, 2021, "Spectroscopic fingerprints of gapped quantum spin liquids, both conventional and fractonic," Phys. Rev. Res. **3**, 013254.
Nandkishore, R. M., and M. Hermele, 2019, "Fractons," Annu. Rev. Condens. Matter Phys. **10**, 295–313.
Nelson, D. R., T. Piran, and S. Weinberg, 1989, Eds., *Statistical Mechanics of Membranes and Interfaces*, 2nd ed. (World Scientific, Singapore).
Nguyen, D., A. Gromov, and S. Moroz, 2020, "Fracton-elasticity duality of two-dimensional superfluid vortex crystals: Defect interactions and quantum melting," SciPost Phys. **9**, 076.
O'Hern, C. S., and T. C. Lubensky, 1998, "Nonlinear elasticity of the sliding columnar phase," Phys. Rev. E **58**, 5948.
O'Hern, C. S., L. E. Silbert, A. J. Liu, and S. R. Nagel, 2003, "Jamming at zero temperature and zero applied stress: The epitome of disorder," Phys. Rev. E **68**, 011306.
Pai, S., and M. Pretko, 2018, "Fractonic line excitations: An inroad from three-dimensional elasticity theory," Phys. Rev. B **97**, 235102.
Pai, S., M. Pretko, and R. Nandkishore, 2019, "Localization in Fractonic Random Circuits," Phys. Rev. X **9**, 021003.
Peskin, M. E., 1978, "Mandelstam–'t Hooft duality in Abelian lattice models," Ann. Phys. (N.Y.) **113**, 122–152.
Prem, A., J. Haah, and R. Nandkishore, 2017, "Glassy quantum dynamics in translation invariant fracton models," Phys. Rev. B **95**, 155133.
Prem, A., M. Pretko, and R. Nandkishore, 2018, "Emergent phases of fractonic matter," Phys. Rev. B **97**, 085116.
Prem, A., S. Vijay, Y. Z. Chou, M. Pretko, and R. M. Nandkishore, 2018, "Pinch point singularities of tensor spin liquids," Phys. Rev. B **98**, 165140.
Pretko, M., 2017a, "Subdimensional particle structure of higher rank U(1) spin liquids," Phys. Rev. B **95**, 115139.
Pretko, M., 2017b, "Generalized electromagnetism of subdimensional particles," Phys. Rev. B **96**, 035119.
Pretko, M., 2017c, "Finite-temperature screening of U(1) fractons," Phys. Rev. B **96**, 115102.
Pretko, M., 2017d, "Emergent gravity of fractons: Mach's principle revisited," Phys. Rev. D **96**, 024051.
Pretko, M., 2017e, "Higher-spin Witten effect and two-dimensional fracton phases," Phys. Rev. B **96**, 125151.
Pretko, M., 2018, "The fracton gauge principle," Phys. Rev. B **98**, 115134.
Pretko, M., X. Chen, and Y. You, 2020, "Fracton phases of matter," Int. J. Mod. Phys. A **35**, 2030003.
Pretko, M., and L. Radzihovsky, 2018a, "Fracton-Elasticity Duality, Phys. Rev. Lett. **120**, 195301.
Pretko, M., and L. Radzihovsky, 2018b, "Symmetry-Enriched Fracton Phases from Supersolid Duality," Phys. Rev. Lett. **121**, 235301.
Pretko, M., Z. Zhai, and L. Radzihovsky, 2019, "Crystal-to-fracton tensor gauge theory dualities," Phys. Rev. B **100**, 134113.
Qi, M., L. Radzihovsky, and M. Hermele, 2021, "Fracton phases via exotic higher-form symmetry-breaking," Ann. Phys. (N.Y.) **424**, 168360.
Radzihovsky, L., 2011, "Fluctuations and phase transitions in Larkin-Ovchinnikov liquid-crystal states of a population-imbalanced resonant Fermi gas," Phys. Rev. A **84**, 023611.
Radzihovsky, L., 2020, "Quantum Smectic Gauge Theory," Phys. Rev. Lett. **125**, 267601.
Radzihovsky, L., and S. Choi, 2009, "*P*-Wave Resonant Bose Gas: A Finite-Momentum Spinor Superfluid," Phys. Rev. Lett. **103**, 095302.
Radzihovsky, L., and A. T. Dorsey, 2002, "Theory of Quantum Hall Nematics," Phys. Rev. Lett. **88**, 216802.
Radzihovsky, L., and M. Hermele, 2020, "Fractons from Vector Gauge Theory," Phys. Rev. Lett. **124**, 050402.
Radzihovsky, L., and A. Vishwanath, 2009, "Quantum Liquid Crystals in an Imbalanced Fermi Gas: Fluctuations and Fractional Vortices in Larkin-Ovchinnikov States," Phys. Rev. Lett. **103**, 010404.
Radzihovsky, Leo, 1995, "Self-consistent theory of normal-to-superconductor transition," Europhys. Lett. **29**, 227.
Radzihovsky, Leo, 2022, "Lifshitz gauge duality," arXiv:2210.03127.
Radzihovsky, Leo, and John Toner, 1995, "A New Phase of Tethered Membranes: Tubules," Phys. Rev. Lett. **75**, 4752.
Radzihovsky, Leo, and John Toner, 1998, "Elasticity, shape fluctuations and phase transitions in the new tubule phase of anisotropic tethered membranes," Phys. Rev. E **57**, 1832–1863.
Rudelius, T., N. Seiberg, and S. H. Shao, 2021, "Fractons with twisted boundary conditions and their symmetries," Phys. Rev. B **103**, 195113.
Sanyal, S., A. Wietek, and J. Sous, 2022, "Unidirectional subsystem symmetry in a hole-doped honeycomb-lattice Ising magnet," arXiv:2210.00012.
Savary, Lucile, and Leon Balents, 2017, "Quantum spin liquids: A review," Rep. Prog. Phys. **80**, 016502.
Schreiber, K. A., and G. A. Csáthy, 2020, "Competition of pairing and nematicity in the two-dimensional electron gas," Annu. Rev. Condens. Matter Phys. **11**, 17.

Seiberg, N., and S. H. Shao, 2021, "Exotic Zn symmetries, duality, and fractons in 3 + 1-dimensional quantum field theory," SciPost Phys. **10**, 003.

Seung, H. S., and David R. Nelson, 1988, "Defects in flexible membranes with crystalline order," Phys. Rev. A **38**, 1005.

Shi, B., and Y.-M. Lu, 2017, "Decipher the nonlocal entanglement entropy of fracton topological orders," arXiv:1705.09300.

Shirley, W., K. Slagle, and X. Chen, 2019, "Universal entanglement signatures of foliated fracton phases," SciPost Phys. **6**, 015.

Slagle, K., and Y. B. Kim, 2017a, "Fracton topological order from nearest-neighbor two-spin interactions and dualities," Phys. Rev. B **96**, 165106.

Slagle, K., and Y. B. Kim, 2017b, "Quantum field theory of X-cube fracton topological order and robust degeneracy from geometry," Phys. Rev. B **96**, 195139.

Slagle, K., A. Prem, and M. Pretko, 2019, "Symmetric tensor gauge theories on curved spaces," Ann. Phys. (N.Y.) **410**, 167910.

Sous, J., and M. Pretko, 2020a, "Fractons from polarons," Phys. Rev. B **102**, 214437.

Sous, J., and M. Pretko, 2020b, "Fractons from frustration in hole-doped antiferromagnets," npj Quantum Mater. **5**, 1–6.

Stahl, C., E. Lake, and R. Nandkishore, 2022, "Spontaneous breaking of multipole symmetries," Phys. Rev. B **105**, 155107.

Surowka, P., 2021, "Dual gauge theory formulation of planar quasicrystal elasticity and fractons," Phys. Rev. B **103**, L201119.

Tranquada, J. M., J. D. Axe, N. Ichikawa, A. R. Moodenbaugh, Y. Nakamura, and S. Uchida, 1997, "Coexistence of, and Competition between, Superconductivity and Charge-Stripe Order in LaNdSrCuO," Phys. Rev. Lett. **78**, 338.

Verresen, R., N. Tantivasadakarn, and A. Vishwanath, 2021, "Efficiently preparing Schrodinger's cat, fractons and non-Abelian topological order in quantum devices," arXiv:2112.03061.

Vijay, S., 2017, "Isotropic layer construction and phase diagram for fracton topological phases," arXiv:1701.00762.

Vijay, S., and L. Fu, 2017, "A generalization of non-Abelian anyons in three dimensions," arXiv:1706.07070.

Vijay, S., J. Haah, and L. Fu, 2015, "A new kind of topological quantum order: A dimensional hierarchy of quasiparticles built from stationary excitations," Phys. Rev. B **92**, 235136.

Vijay, S., J. Haah, and L. Fu, 2016, "Fracton topological order, generalized lattice gauge theory and duality," Phys. Rev. B **94**, 235157.

Vishwanath, A., L. Balents, and T. Senthil, 2004, "Quantum criticality and deconfinement in phase transitions between valence bond solids," Phys. Rev. B **69**, 224416.

Wen, X. G., 2020, "Systematic construction of gapped nonliquid states," Phys. Rev. Res. **2**, 033300.

Williamson, D. J., 2016, "Fractal symmetries: Ungauging the cubic code," Phys. Rev. B **94**, 155128.

Xing, Xiangjun, and Leo Radzihovsky, 2003, "Universal Elasticity and Fluctuations of Nematic Gels," Phys. Rev. Lett. **90**, 168301.

Xing, Xiangjun, and Leo Radzihovsky, 2008, "Nonlinear elasticity, fluctuations and heterogeneity of nematic elastomers," Ann. Phys. (N.Y.) **323**, 105–203.

Xu, C., and P. Horova, 2010, "Emergent gravity at a Lifshitz point from a Bose liquid on the lattice," Phys. Rev. D **81**, 104033.

Yan, H., 2019, "Hyperbolic fracton model, subsystem symmetry, and holography," Phys. Rev. B **99**, 155126.

Yan, H., O. Benton, L. D. C. Jaubert, and N. Shannon, 2020, "Rank-2 U(1) Spin Liquid on the Breathing Pyrochlore Lattice," Phys. Rev. Lett. **124**, 127203.

Yoshida, B., 2013, "Exotic topological order in fractal spin liquids," Phys. Rev. B **88**, 125122.

Young, A. P., 1979, "Melting and the vector Coulomb gas in two dimensions," Phys. Rev. B **19**, 1855.

Zechmann, Philip, Ehud Altman, Michael Knap, and Johannes Feldmeier, 2022, "Fractonic Luttinger liquids and supersolids in a constrained Bose-Hubbard model," arXiv:2210.11072.

Zhai, Hui, 2015, "Degenerate quantum gases with spin-orbit coupling: A review," Rep. Prog. Phys. **78**, 026001.

Zhai, Z. Z., and L. Radzihovsky, 2021, "Fractonic gauge theory of smectics," Ann. Phys. (N.Y.) **435**, 168509.

Zhai, Zhengzheng, and Leo Radzihovsky, 2019, "Two-dimensional melting via sine-Gordon duality," Phys. Rev. B **100**, 094105.